

# Leptoquark Pair Production in Hadronic Interactions

Johannes Blümlein<sup>1</sup>, Edward Boos<sup>1,2</sup>, and Alexander Kryukov<sup>1,2</sup>

<sup>1</sup>*DESY -Zeuthen,*

*Platanenallee 6, D-15735 Zeuthen, Germany*

<sup>2</sup>*Institute of Nuclear Physics, Moscow State University,  
RU-119899 Moscow, Russia*

## Abstract

The scalar and vector leptoquark pair production cross sections in hadronic collisions are calculated. In a model independent analysis we consider the most general  $C$  and  $P$  conserving couplings of gluons to both scalar and vector leptoquarks described by an effective low-energy Lagrangian which obeys  $SU(3)_c$  invariance. Analytical expressions are derived for the differential and integral scattering cross sections including the case of anomalous vector leptoquark couplings,  $\kappa_G$  and  $\lambda_G$ , to the gluon field. Numerical predictions are given for the kinematic range of the TEVATRON and LHC. The pair production cross sections are also calculated for the resolved photon contributions to  $ep \rightarrow e\bar{\Phi}\Phi X$  at HERA and LEP  $\otimes$  LHC, and for the process  $\gamma\gamma \rightarrow \Phi\bar{\Phi}X$  at possible future  $e^+e^-$  linear colliders and  $\gamma\gamma$  colliders. Estimates of the search potential for scalar and vector leptoquarks at present and future high energy colliders are given.

# 1 Introduction

In many extensions of the Standard Model new bosons are predicted which carry both lepton and baryon number [1]. There is indeed a close relation between these quantum numbers in the Standard Model since the triangle anomalies are cancelled by the requirement

$$\sum_n Q_n^2 (Q_L - Q_R)_n = 0 \quad (1)$$

for each fermion family, which renders the theory renormalizable. Here  $Q_n$ ,  $Q_{Ln}$ , and  $Q_{Rn}$  denote the electromagnetic, left-, and right-handed neutral current charges, respectively. Leptoquark states emerge naturally as the gauge bosons in Grand Unified Theories [2]. In these scenarios their couplings are not baryon number conserving and their masses are situated in the range  $M_\Phi \gtrsim 10^{15}$  GeV. On the other hand, leptoquarks with B- and L-conserving couplings may exist in the mass range accessible at high energy colliders. These states will be considered in the present paper. They may be either sought through virtual effects in low energy processes, from which already severe constraints on their fermionic couplings were derived [3], or searched for at high energy colliders as at LEP [4], HERA [5], and TEVATRON [6]. These searches constrained further the allowed mass and coupling ranges being limited by other experiments [7] previously. At present the most stringent constraints come from the TEVATRON and exclude leptoquarks associated with the first and second family with masses in the range  $M_\Phi \lesssim O(100)$  GeV [8]. For the third generation scalar leptoquarks currently the mass range  $M_\Phi < 45$  GeV is excluded.

In the case of single leptoquark production the scattering cross sections are always proportional to one of the fermionic couplings [9],  $\lambda_{lq}$ , which are constrained to be rather small from low energy processes up to masses of  $M_\Phi \sim O(1 \text{ TeV})$ <sup>1</sup>. Thus the search limits *always* lead to combined bounds on the couplings  $\lambda_{lq}$  and the leptoquark masses. For leptoquark pair production, however, the small size of the fermionic couplings does not severely constrain the scattering cross sections due to the finite bosonic contributions. The strength of the leptoquark couplings to the gauge bosons,  $\gamma$ ,  $g$ ,  $W^\pm$ , and  $Z^0$ , is determined by the coupling constant of the respective gauge field up to eventual anomalous contributions in the case of vector leptoquarks, which are described by the parameters  $\kappa_A$  and  $\lambda_A$ , with  $A = \gamma, g, W^\pm$ , and  $Z^0$ . As will be shown for the hadronic contributions to the different scattering cross sections, a combination of anomalous couplings  $(\kappa_G, \lambda_G)$  exists for which they become minimal. Therefore one may constrain the allowed mass ranges for leptoquarks *directly*. As will be shown, the corresponding minimizing couplings are in general *not* those of the Yang-Mills type or the minimal vector boson couplings.

In the present paper the cross sections for scalar and vector leptoquark pair production in hadronic interactions are calculated. They apply for  $p\bar{p}$  and  $pp$  scattering at the TEVATRON and LHC, respectively, but also for hadronic interactions at  $ep$ ,  $e^+e^-$ , and  $\gamma\gamma$  colliders. In the latter cases they emerge as the resolved photon contributions which accompany the respective direct photon processes [11]–[13].

The paper is organized as follows. In section 2 the basic notations are introduced. Section 3 contains the derivation of the partonic scattering cross sections for scalar and vector leptoquark pair production including the anomalous couplings  $\kappa_A$  and  $\lambda_A$ . Here it is also shown how the scattering cross sections for the scalar and the vector case, in the absence of anomalous couplings, can be obtained using factorization relations of the amplitude. The hadronic production cross sections are derived in section 4. For  $ep$ ,  $e^+e^-$ , and  $\gamma\gamma$  scattering the direct photon contributions

---

<sup>1</sup>For even higher masses the fermion couplings of leptoquarks can still be of the order  $\lambda_{lq} \sim e$ . Single production at proton colliders has been studied in [10] recently.

calculated previously [11]–[13] are added to obtain a complete description. The numerical results are presented in section 5<sup>2</sup> and section 6 contains the conclusions. The Feynman rules used in the present calculation are summarized in Appendix A. Appendix B contains the coefficients which describe the differential and integrated pair production cross sections for vector leptoquarks in the presence of anomalous couplings.

## 2 Basic Notations

Following earlier investigations [11]–[13],[15] we consider the class of leptoquarks introduced in [16]. The fermionic couplings of these states are dimensionless, baryon and lepton number conserving, family–diagonal, and  $SU(3)_c \times SU(2)_L \times U(1)_Y$  invariant. These leptoquarks are color triplets. As outlined in ref. [15], these conditions do widely induce also the couplings to the gauge bosons of the Standard Model. For the scalar states their bosonic couplings are determined completely. In the case of vector leptoquarks, the Yang–Mills type couplings may be supplemented by anomalous couplings which are specified by two parameters  $\kappa_A$  and  $\lambda_A$ . The couplings  $\kappa_A$  and  $\lambda_A$ , corresponding to different gauge fields, are not generally related. The hadronic processes depend on the parameters  $\kappa_G$  and  $\lambda_G$  only. Since most of the fermionic couplings  $\lambda_{lq}$  of the leptoquarks are bounded to be very small in the mass range up to  $\mathcal{O}(1 \text{ TeV})$  [3], we will neglect their contribution in the following and consider pair production through bosonic couplings only<sup>3</sup>.

The effective Lagrangian describing the interaction of the scalar and vector leptoquarks with gluons is given by

$$\mathcal{L} = \mathcal{L}_S^g + \mathcal{L}_V^g, \quad (2)$$

where

$$\mathcal{L}_S^g = \sum_{\text{scalars}} \left[ \left( D_{ij}^\mu \Phi^j \right)^\dagger \left( D_\mu^{ik} \Phi_k \right) - M_S^2 \Phi^{i\dagger} \Phi_i \right], \quad (3)$$

$$\mathcal{L}_V^g = \sum_{\text{vectors}} \left\{ -\frac{1}{2} G_{\mu\nu}^{i\dagger} G_i^{\mu\nu} + M_V^2 \Phi_\mu^{i\dagger} \Phi_i^\mu - i g_s \left[ (1 - \kappa_G) \Phi_\mu^{i\dagger} t_{ij}^a \Phi_\nu^j \mathcal{G}_a^{\mu\nu} + \frac{\lambda_G}{M_V^2} G_{\sigma\mu}^{i\dagger} t_{ij}^a G_\nu^{j\mu} \mathcal{G}_a^{\nu\sigma} \right] \right\}. \quad (4)$$

Here,  $g_s$  denotes the strong coupling constant,  $t_a$  are the generators of  $SU(3)_c$ ,  $M_S$  and  $M_V$  are the leptoquark masses, and  $\kappa_G$  and  $\lambda_G$  are the anomalous couplings. The field strength tensors of the gluon and vector leptoquark fields are

$$\begin{aligned} \mathcal{G}_{\mu\nu}^a &= \partial_\mu \mathcal{A}_\nu^a - \partial_\nu \mathcal{A}_\mu^a + g_s f^{abc} \mathcal{A}_{\mu b} \mathcal{A}_{\nu c}, \\ G_{\mu\nu}^i &= D_\mu^{ik} \Phi_{\nu k} - D_\nu^{ik} \Phi_{\mu k}, \end{aligned} \quad (5)$$

with the covariant derivative given by

$$D_\mu^{ij} = \partial_\mu \delta^{ij} - i g_s t_a^{ij} \mathcal{A}_\mu^a. \quad (6)$$

The parameters  $\kappa_G$  and  $\lambda_G$  are assumed to be real. They are related to the anomalous 'magnetic' moment  $\mu_V$  and 'electric' quadrupole moment  $q_V$  of the leptoquarks in the color field

$$\mu_{V,G} = \frac{g_s}{2M_V} (2 - \kappa_G + \lambda_G),$$

---

<sup>2</sup>The code for the different processes can be obtained on request from [blumlein@ifh.de](mailto:blumlein@ifh.de). A detailed description of the code LQPAIR 1.0 is given in [14].

<sup>3</sup> The hadronic pair production cross sections for leptoquarks of different flavor  $\Phi_1 \bar{\Phi}_2$  or  $\Phi_1 \Phi_2$  is possible through quark or quark–antiquark scattering and depends on the fermionic couplings as  $\propto \lambda_{lq}^4$ .

$$q_{V,G} = -\frac{g_s}{M_V^2} (1 - \kappa_G - \lambda_G). \quad (7)$$

Since we wish to keep the analysis as model independent as possible we assume that these quantities are independent. At present there are no direct bounds on the parameters  $\kappa_G$  and  $\lambda_G$ . Below we will consider the range of  $|\kappa_G|, |\lambda_G| \leq 1$ . The hadronic production cross sections are found to vary significantly for parameters in this range. As will be shown, searches at the TEVATRON will be able to constrain this range further. The above choice covers both the cases of Yang–Mills type couplings,  $\kappa_G = \lambda_G = 0$ , and the minimal vector couplings,  $\kappa_G = 1, \lambda_G = 0$ .

The Feynman rules relevant for the processes studied in the present paper are summarized in Appendix A.

### 3 Partonic Cross Sections

Before we study the pair production cross sections for leptiquarks at different colliders we present the partonic cross sections. The diagrams of the contributing subprocesses  $gg \rightarrow \Phi\bar{\Phi}$  and  $q\bar{q} \rightarrow \Phi\bar{\Phi}$  are shown in figure 1 and 2. Let us first consider the case of vanishing anomalous couplings, i.e. the simplified situation in which the production cross sections depend on the gauge coupling *only*.

In non-Abelian gauge theories the amplitudes for a series of  $2 \rightarrow 2$  scattering processes can be factorized into a group and a Lorentz part [17]. As will be shown this applies to  $\mathcal{M}(gg \rightarrow \Phi_S\bar{\Phi}_S)$  and  $\mathcal{M}(gg \rightarrow \Phi_V\bar{\Phi}_V)$  for the special case of vanishing anomalous vector couplings  $\kappa_G = \lambda_G \equiv 0$ . This representation also yields a particularly simple result for the differential cross sections in comparison with expressions obtained otherwise [18, 19]. The former case has been dealt with in ref. [17] using this method, however, the scattering cross section obtained disagrees with other results [18]. Therefore we will recalculate the cross sections for both cases showing the factorization of the group factor and the Lorentz part in detail before deriving the more general result for finite anomalous couplings  $\kappa_G$  and  $\lambda_G$ .

#### 3.1 Factorization Relations

We use a physical gauge for the gluon fields. The gluon polarization vectors  $\varepsilon_g$  obey  $\varepsilon_g \cdot p_g = 0$  and  $\sum_\lambda \varepsilon_g^\mu(\lambda)\varepsilon_g^{\nu*}(\lambda) = -g^{\mu\nu} + p_g^\mu p_g^\nu / p_g \cdot p_g$ . The matrix elements for the above processes can be written as

$$\mathcal{M}^{S,V} = \sum_p g_s^2 G_p \frac{T_p^{S,V}}{C_p}, \quad (8)$$

with  $p = s, t, u$  the channel index,  $C_s = s, C_t \equiv \hat{t} = t - M_\Phi^2$ , and  $C_u \equiv \hat{u} = u - M_\Phi^2$ . The numerators in the matrix element have been written in terms of the respective group factors  $G_p$  and the Lorentz parts  $T_p^{S,V}$ . The following relations are valid.

$$C_s + C_u + C_t = 0, \quad (9)$$

$$G_t - G_u = G_s, \quad (10)$$

$$\hat{T}_t - \hat{T}_u = T_s + \Delta. \quad (11)$$

Since  $G_t = (t^a t^b)_{ij}$ ,  $G_u = (t^b t^a)_{ij}$ , and  $G_s = if_{abc} t_{ij}^c$ , eq. (10) is the commutation relation of the generators of  $SU(3)_c$ . The Lorentz terms  $\hat{T}_{t,u}$  consist out of the  $t$  and  $u$  channel terms supplemented by the parts of the sea–gull diagram (see figure 1) corresponding to the group

factor  $G_t$  and  $G_u$ , respectively. The contributions to the Lorentz parts  $T_s, \hat{T}_t$  and  $\hat{T}_u$  are given in table 1 for the scalar and vector case. One finds that

$$\Delta = p_1 \cdot \varepsilon(p_1) A + p_2 \cdot \varepsilon(p_2) B \equiv 0, \quad (12)$$

with  $\varepsilon(p_i)$  the gluon polarization vectors. These relations result into

$$|\mathcal{M}|^2 = |G|^2 |\mathcal{M}_A|^2 = |G|^2 g_s^2 \left| \frac{\hat{T}_t}{C_t} + \frac{\hat{T}_u}{C_u} \right|^2. \quad (13)$$

$\mathcal{M}_A$  has thus the form of an Abelian amplitude. Since the leptoquarks described by (2) are color triplets or antitriplets one obtains

$$|G|^2 = \left| \frac{C_u G_t + C_t G_u}{C_s} \right|^2 = \frac{16}{3} \frac{\hat{u}^2 + \hat{t}^2}{s^2} - \frac{4}{3} \frac{\hat{u}\hat{t}}{s^2} = 4 \left( \frac{4}{3} - 3 \frac{\hat{u}\hat{t}}{s^2} \right). \quad (14)$$

	Scalar Field	Vector Field, $\kappa_G = \lambda_G = 0$
$T_s$	$-(q_1 - q_2) \cdot \varepsilon_1 (2p_1 + p_2) \cdot \varepsilon_2$ $+(q_1 - q_2) \cdot \varepsilon_2 (2p_2 + p_1) \cdot \varepsilon_1$ $+(\hat{u} - \hat{t}) \varepsilon_1 \cdot \varepsilon_2$	$\varepsilon_1 \cdot \varepsilon_2 \varepsilon_1 \cdot \varepsilon_2 (\hat{u} - \hat{t})$ $+4\varepsilon_1 \cdot \varepsilon_2 (-p_1 \cdot \varepsilon_1 p_2 \cdot \varepsilon_2 + p_1 \cdot \varepsilon_2 p_2 \cdot \varepsilon_1)$ $-4\varepsilon_1 \cdot \varepsilon_1 (p_1 \cdot \varepsilon_2 q_1 \cdot \varepsilon_2 + p_1 \cdot \varepsilon_2 q_2 \cdot \varepsilon_2 + p_2 \cdot \varepsilon_2 q_1 \cdot \varepsilon_2 + p_2 \cdot \varepsilon_2 q_2 \cdot \varepsilon_2)$ $+4\varepsilon_1 \cdot \varepsilon_2 (p_1 \cdot \varepsilon_1 q_1 \cdot \varepsilon_2 + p_1 \cdot \varepsilon_1 q_2 \cdot \varepsilon_2 + p_2 \cdot \varepsilon_1 q_1 \cdot \varepsilon_2 + p_2 \cdot \varepsilon_1 q_2 \cdot \varepsilon_2)$ $+4\varepsilon_2 \cdot \varepsilon_1 (p_1 \cdot \varepsilon_2 q_1 \cdot \varepsilon_1 + p_1 \cdot \varepsilon_2 q_2 \cdot \varepsilon_1 + p_2 \cdot \varepsilon_2 q_1 \cdot \varepsilon_1 + p_2 \cdot \varepsilon_2 q_2 \cdot \varepsilon_1)$ $-4\varepsilon_2 \cdot \varepsilon_2 (p_1 \cdot \varepsilon_1 q_1 \cdot \varepsilon_1 + p_1 \cdot \varepsilon_1 q_2 \cdot \varepsilon_1 + p_2 \cdot \varepsilon_1 q_1 \cdot \varepsilon_1 + p_2 \cdot \varepsilon_1 q_2 \cdot \varepsilon_1)$ $+4\varepsilon_1 \cdot \varepsilon_2 (-q_1 \cdot \varepsilon_1 q_2 \cdot \varepsilon_2 + q_1 \cdot \varepsilon_2 q_2 \cdot \varepsilon_1)$
$\hat{T}_t$	$(2q_1 - p_1) \cdot \varepsilon_1 (p_2 - 2q_2) \cdot \varepsilon_2 - \hat{t} \varepsilon_1 \cdot \varepsilon_2$	$-\varepsilon_1 \cdot \varepsilon_2 \varepsilon_1 \cdot \varepsilon_2 \hat{t}$ $+2(\varepsilon_1 \cdot \varepsilon_1 \varepsilon_2 \cdot \varepsilon_2 \hat{u} + \varepsilon_1 \cdot \varepsilon_2 \varepsilon_2 \cdot \varepsilon_1 \hat{t})$ $-4(\varepsilon_1 \cdot \varepsilon_2 p_1 \cdot \varepsilon_1 p_2 \cdot \varepsilon_2 + \varepsilon_1 \cdot \varepsilon_2 q_1 \cdot \varepsilon_1 q_2 \cdot \varepsilon_2)$ $+4(\varepsilon_1 \cdot \varepsilon_2 p_1 \cdot \varepsilon_1 q_2 \cdot \varepsilon_2 + \varepsilon_2 \cdot \varepsilon_1 p_2 \cdot \varepsilon_2 q_1 \cdot \varepsilon_1)$ $-4\varepsilon_1 \cdot \varepsilon_1 (p_1 \cdot \varepsilon_2 q_2 \cdot \varepsilon_2 + p_2 \cdot \varepsilon_2 q_1 \cdot \varepsilon_2 + p_2 \cdot \varepsilon_2 q_2 \cdot \varepsilon_2)$ $-4\varepsilon_2 \cdot \varepsilon_2 (p_1 \cdot \varepsilon_1 q_1 \cdot \varepsilon_1 + p_1 \cdot \varepsilon_1 q_2 \cdot \varepsilon_1 + p_2 \cdot \varepsilon_1 q_1 \cdot \varepsilon_1)$
$\hat{T}_u$	$(2q_1 - p_2) \cdot \varepsilon_1 (p_1 - 2q_2) \cdot \varepsilon_2 - \hat{u} \varepsilon_1 \cdot \varepsilon_2$	$-\varepsilon_1 \cdot \varepsilon_2 \varepsilon_1 \cdot \varepsilon_2 \hat{u}$ $+2(\varepsilon_1 \cdot \varepsilon_1 \varepsilon_2 \cdot \varepsilon_2 \hat{u} + \varepsilon_1 \cdot \varepsilon_2 \varepsilon_2 \cdot \varepsilon_1 \hat{t})$ $-4(\varepsilon_1 \cdot \varepsilon_2 p_1 \cdot \varepsilon_2 p_2 \cdot \varepsilon_1 + \varepsilon_1 \cdot \varepsilon_2 q_1 \cdot \varepsilon_2 q_2 \cdot \varepsilon_1)$ $+4(\varepsilon_1 \cdot \varepsilon_1 p_1 \cdot \varepsilon_2 q_1 \cdot \varepsilon_2 + \varepsilon_2 \cdot \varepsilon_2 p_2 \cdot \varepsilon_1 q_2 \cdot \varepsilon_2)$ $-4\varepsilon_1 \cdot \varepsilon_2 (p_1 \cdot \varepsilon_1 q_1 \cdot \varepsilon_2 + p_2 \cdot \varepsilon_1 q_1 \cdot \varepsilon_2 + p_2 \cdot \varepsilon_1 q_2 \cdot \varepsilon_2)$ $-4\varepsilon_2 \cdot \varepsilon_1 (p_1 \cdot \varepsilon_2 q_1 \cdot \varepsilon_1 + p_1 \cdot \varepsilon_2 q_2 \cdot \varepsilon_1 + p_2 \cdot \varepsilon_2 q_2 \cdot \varepsilon_1)$

Table 1:  $stu$  contributions to the Lorentz part of the scattering amplitudes  $gg \rightarrow \Phi\bar{\Phi}$ . The polarization vectors of the vector field are denoted by  $\varepsilon_{1,2}$ .

The Lorentz parts of the amplitude yield

$$|\mathcal{M}_A^S|^2 = 8g_s^4 \left[ 1 - 2 \frac{sM_S^2}{\hat{t}\hat{u}} + 2 \left( \frac{sM_S^2}{\hat{t}\hat{u}} \right)^2 \right], \quad (15)$$

and

$$|\mathcal{M}_A^V|^2 = 8g_s^4 \left[ 3 - 2 \left( 2 - \frac{s^2}{\hat{t}\hat{u}} \right) \frac{s^2}{\hat{t}\hat{u}} - 6 \left( 1 - \frac{M_V^2 s}{\hat{t}\hat{u}} \right) \frac{M_V^2 s}{\hat{t}\hat{u}} \right]. \quad (16)$$

Comparing (13) with other results obtained in earlier calculations, we agree with the scattering cross sections for scalar pair production derived in [18] but disagree with those found in [17, 20, 21]<sup>4</sup>. Our result for pair production of vector color triplets agrees with that given in [19, 21]<sup>5</sup>.

### 3.2 Scalar Leptoquarks

The differential and integral pair production cross sections for  $gg$  and  $q\bar{q}$  scattering are

$$\begin{aligned} \frac{d\hat{\sigma}_{S\bar{S}}^{gg}}{d\cos\theta} &= \frac{\pi\alpha_s^2}{6\hat{s}}\beta \left\{ \frac{1}{32} [25 + 9\beta^2 \cos^2\theta - 18\beta^2] \right. \\ &\quad \left. - \frac{1}{16} \frac{(25 - 34\beta^2 + 9\beta^4)}{1 - \beta^2 \cos^2\theta} + \frac{(1 - \beta^2)^2}{(1 - \beta^2 \cos^2\theta)^2} \right\}, \end{aligned} \quad (17)$$

$$\hat{\sigma}_{S\bar{S}}^{gg} = \frac{\pi\alpha_s^2}{96\hat{s}} \left\{ \beta (41 - 31\beta^2) - (17 - 18\beta^2 + \beta^4) \log \left| \frac{1 + \beta}{1 - \beta} \right| \right\}, \quad (18)$$

and

$$\frac{d\hat{\sigma}_{S\bar{S}}^{q\bar{q}}}{d\cos\theta} = \frac{\pi\alpha_s^2}{18\hat{s}}\beta^3 \sin^2\theta, \quad (19)$$

$$\hat{\sigma}_{S\bar{S}}^{q\bar{q}} = \frac{2\pi\alpha_s^2}{27\hat{s}}\beta^3, \quad (20)$$

with  $\alpha_s = g_s^2/4\pi$ ,  $\beta = \sqrt{1 - 4M_\Phi^2/\hat{s}}$ ,  $\hat{s}^{1/2}$  the cms energy and  $\theta$  the leptoquark scattering angle in the parton-parton cms. All quark flavors have been dealt with as massless<sup>6</sup>. Eqs. (17, 18) result from (13) directly. Eqs. (19,20) are known for a long time, cf. ref. [26].

### 3.3 Vector Leptoquarks

While for the case of vanishing anomalous couplings,  $\kappa_G = \lambda_G \equiv 0$ , the pair production cross section follows from eq. (13) it cannot be derived by the technique discussed in section 3.1 for finite anomalous couplings because eq. (12) does not hold. For the general case we have performed the calculation of  $|\mathcal{M}_{q,g}^V|^2$  by CompHEP [27] in the Feynman gauge<sup>7</sup>. We also checked gauge invariance explicitly using FORM [28] in the  $R_\xi$  gauge with a free gauge parameter. For these calculations, the diagrams in figure 1 must be supplemented by an initial state ghost contribution.

<sup>4</sup> We checked that the difference in  $\hat{\sigma}_{S\bar{S}}^{gg}$  in ref. [20] could be explained by leaving out the ghost term in the Feynman gauge. The result obtained in ref. [22] agrees with that given in [20] and was used to derive numerical results. Later the same authors revised this expression, see [23], and agree with eq. (18). Since ref. [11] in [24] refers to two *different* expressions for  $\sigma(gg \rightarrow \Phi_s \bar{\Phi}_s)$  it remains unclear on which relation the numerical calculation presented was based.

<sup>5</sup> A numerical illustration of this relation has been given in [25] for the gluonic contributions recently.

<sup>6</sup> This is a sufficient approximation in the mass and energy range  $M_\Phi > 40$  GeV and  $\sqrt{S} \geq 300$  GeV considered in the present paper.

<sup>7</sup> The Feynman rules given in appendix A have been implemented into CompHEP as a new model.

The differential and integral pair production cross sections for  $gg$  scattering are

$$\frac{d\hat{\sigma}_{V\bar{V}}^{gg}}{d\cos\theta} = \frac{\pi\alpha_s^2}{192\hat{s}}\beta\sum_{i=0}^{14}\chi_i^g(\kappa_G, \lambda_G)\frac{F_i(\hat{s}, \beta, \cos\theta)}{(1-\beta^2\cos^2\theta)^2}, \quad (21)$$

with

$$\begin{aligned} \sum_{i=0}^{14}\chi_i^g(\kappa_G, \lambda_G)F_i &= F_0 + \kappa_GF_1 + \lambda_GF_2 + \kappa_G^2F_3 + \kappa_G\lambda_GF_4 \\ &+ \lambda_G^2F_5 + \kappa_G^3F_6 + \kappa_G^2\lambda_GF_7 + \kappa_G\lambda_G^2F_8 + \lambda_G^3F_9 \\ &+ \kappa_G^4F_{10} + \kappa_G^3\lambda_GF_{11} + \kappa_G^2\lambda_G^2F_{12} + \kappa_G\lambda_G^3F_{13} + \lambda_G^4F_{14}, \end{aligned} \quad (22)$$

$$\hat{\sigma}_{V\bar{V}}^{gg} = \frac{\pi\alpha_s^2}{96M_V^2}\sum_{i=0}^{14}\chi_i^g(\kappa_G, \lambda_G)\tilde{F}_i(\hat{s}, \beta), \quad (23)$$

$$\tilde{F}_i = \frac{M_V^2}{\hat{s}}\int_0^\beta d\xi\frac{F_i(\xi = \beta\cos\theta)}{(1-\xi^2)^2}. \quad (24)$$

The functions  $F_i(\hat{s}, \beta, \cos\theta)$  and  $\tilde{F}_i(\hat{s}, \beta)$  are obtained after a lengthy calculation and are given in appendix B. Similar to the case of  $\gamma g$  [11] and  $\gamma\gamma$  [13] scattering, the contributions *linear* in either  $\kappa_G$  or  $\lambda_G$  do not contain unitarity violating pieces  $\propto \hat{s}/M_V^2$ .

For  $q\bar{q}$  scattering the cross section reads

$$\frac{d\hat{\sigma}_{V\bar{V}}^{q\bar{q}}}{d\cos\theta} = \frac{2\pi\alpha_s^2}{9M_V^2}\beta^3\sum_{i=0}^5\chi_i^q(\kappa_G, \lambda_G)G_i(\hat{s}, \beta, \cos\theta), \quad (25)$$

with

$$\sum_{i=0}^5\chi_i^q(\kappa_G, \lambda_G)G_i = G_0 + \kappa_G G_1 + \lambda_G G_2 + \kappa_G^2 G_3 + \kappa_G\lambda_G G_4 + \lambda_G^2 G_5. \quad (26)$$

The integrated cross section is

$$\hat{\sigma}_{V\bar{V}}^{q\bar{q}} = \frac{4\pi\alpha_s^2}{9M_V^2}\beta^3\sum_{i=0}^5\chi_i^q(\kappa_G, \lambda_G)\tilde{G}_i(\hat{s}, \beta), \quad (27)$$

where

$$\tilde{G}_i = \int_0^1 d\cos\theta G_i(\hat{s}, \beta, \cos\theta). \quad (28)$$

The functions  $G_i(\hat{s}, \beta, \cos\theta)$  and  $\tilde{G}_i(\hat{s}, \beta)$  are listed in appendix B. For  $\lambda_G = 0$  eqs. (25,27) agree with those found in [21] specifying the color factor<sup>8</sup>. Relations for the special cases  $\kappa_G = 0$  [29] and  $\kappa_G = 1$  [15] have been obtained for other reactions previously.

Contrary to the case of gluo-production (23), terms  $\propto \hat{s}/M_V^2$  are contained even in the contribution  $G_0$  because we did not impose a relation between the fermionic and bosonic couplings of the leptoquarks for Yang-Mills type leptoquark-gauge boson couplings. To restore unitarity, graphs with lepton exchange would have to be added for the process  $q\bar{q} \rightarrow \Phi_V\bar{\Phi}_V$ . The value required for the adjusted fermionic couplings, however, would be too large to be consistent with the limits derived in [3]. The Lagrangian (2) is assumed to parametrize leptoquark interactions

<sup>8</sup>Note that this result disagrees with eq. (4) in [25] by a factor of 81/4.

for not too large energies, i.e. in the threshold range. It has to be supplemented by further terms restoring the correct high energy behaviour for  $\hat{s} \gg M_V^2$ . These terms are model dependent and are related to the specific scenario leading to leptoquarks in the mass range of 100 GeV to  $\sim 1$  TeV. Approaching high energies, symmetry breaking scales are passed and the respective Higgs terms contribute.

## 4 Production Cross Sections

Subsequently we will calculate the differential and integral hadronic production cross sections for leptoquark pair production at different colliders. In the present paper we will apply the collinear parton model to describe the initial state of the hard scattering process  $f_i f_j \rightarrow \Phi \bar{\Phi}$ . The densities  $f_i$  are the parton densities in the case of the  $p\bar{p}$  or  $pp$  collisions. For the resolved photon contributions in  $ep$  collisions one of the densities is the probability for finding a quark, antiquark, or gluon in the electron in a neutral current process. These distributions are described by the convolution

$$f_{i/e}(x, \mu^2) = [f_{\gamma/e}(\mu^2) \otimes f_{i/\gamma}(\mu^2)](x), \quad (29)$$

where  $f_{\gamma/e}(x, \mu^2)$  is the photon density in an electron and  $f_{i/\gamma}(x, \mu^2)$  denotes the density of parton  $i$  in the photon. The convolution of the densities is given by

$$[A \otimes B](x) = \int_0^1 \int_0^1 dx_1 dx_2 \delta(x - x_1 x_2) A(x_1) B(x_2). \quad (30)$$

In the same way the parton densities for photoproduction of leptoquark pairs at  $e^+e^-$  colliders are described. For  $\gamma\gamma$  colliders, at which the photon beams are prepared by laser back-scattering, the distribution  $f_{\gamma/e}(z)$  is given by the Compton spectrum  $\phi_C(z)$ , eq. (59).

In  $ep$ ,  $\gamma^*\gamma^*$ , and  $\gamma\gamma$  scattering, in addition to the resolved photon subprocesses, *direct* contributions due to  $\gamma g$  and  $\gamma\gamma$  fusion are present which have been studied in refs. [11] and [12, 13], respectively.

In terms of the *generalized* partonic distributions  $f_i^{(c)}(x_c, \mu^2)$  the differential cross section reads:

$$\frac{d^2\sigma}{d\eta dp_\perp^2} = \int_0^1 dx_a \frac{\sqrt{S} \theta(\hat{s} - 4M_\Phi^2)}{x_a \sqrt{S} - \sqrt{M_\Phi^2 + p_\perp^2} (\text{ch}\eta + \text{sh}\eta)} x_a x_b f_i^{(a)}(x_a, \mu^2) f_j^{(b)}(x_b, \mu^2) \frac{2}{\hat{s}\beta} \frac{d\hat{\sigma}^{ij}(\hat{s}, \hat{t}, \hat{u})}{d\cos\theta}. \quad (31)$$

Here,  $\eta$  denotes the rapidity of one of the leptoquarks,

$$\eta = \frac{1}{2} \ln \left| \frac{E_h + p_{zh}}{E_h - p_{zh}} \right|, \quad (32)$$

with  $E_h$  and  $p_{zh}$  the leptoquark energy and longitudinal momentum.  $p_\perp$  is the transverse momentum in the laboratory frame,  $\hat{s} = x_a x_b s$ , and

$$x_b = \frac{x_a \sqrt{M_\Phi^2 + p_\perp^2} (\text{ch}\eta - \text{sh}\eta)}{x_a \sqrt{s} - \sqrt{M_\Phi^2 + p_\perp^2} (\text{ch}\eta + \text{sh}\eta)}. \quad (33)$$

The Mandelstam variables  $\hat{t}$  and  $\hat{u}$  in the cms are

$$\hat{t} = M_\Phi^2 - x_a \sqrt{s} \sqrt{M^2 + p_\perp^2} (\text{ch}\eta - \text{sh}\eta) = M_\Phi^2 - \frac{\hat{s}}{2} (1 - \beta \cos\theta), \quad (34)$$

$$\hat{u} = M_\Phi^2 - x_b \sqrt{s} \sqrt{M_\Phi^2 + p_\perp^2} (\text{ch}\eta + \text{sh}\eta) = M_\Phi^2 - \frac{\hat{s}}{2} (1 + \beta \cos\theta). \quad (35)$$



The differential cross sections in the partonic sub-systems  $d\hat{\sigma}^{ij}/d\cos\theta$  have been given in eqs. (17,19,21,25) in section 3. The single differential distributions  $d\sigma/d\eta$  and  $d\sigma/dp_\perp^2$  are derived from eq. (31). Eq. (33) constrains the rapidity and  $p_\perp$  ranges to

$$-\frac{1}{2}\log\frac{1+B}{1-B}\leq\eta\leq\frac{1}{2}\log\frac{1+B}{1-B}, \quad (36)$$

$$0\leq p_\perp\leq\frac{\sqrt{s}}{2}\sqrt{\beta^2-\text{th}^2\eta}, \quad (37)$$

where  $B=\sqrt{1-4(M_\Phi^2+p_\perp^2)}/s$ .

Finally the integral cross sections are

$$\sigma(\Phi\bar{\Phi})=\int_0^1\int_0^1dx_adx_bf_i^{(a)}(x_a,\mu^2)f_j^{(b)}(x_b,\mu^2)\hat{\sigma}^{ij}(\hat{s})\theta(\hat{s}-4M_\Phi^2). \quad (38)$$

To be specific, we list the relations for the different contributions to the integrated cross sections for  $pp(p\bar{p})$ ,  $ep$  and  $\gamma\gamma(\gamma^*\gamma^*)$  scattering explicitly below.

## 4.1 $p\bar{p}$ and $pp$ scattering

Here the total cross section consists of contributions from quark–antiquark annihilation and gluon–gluon fusion

$$\sigma_{S,V}^{pp}(s,M_\Phi)=\sigma_{S,V}^{pp;q}(s,M_\Phi)+\sigma_{S,V}^{pp;g}(s,M_\Phi), \quad (39)$$

where

$$\begin{aligned} \sigma_{S,V}^{pp;q}(s,M_\Phi) &= \sum_{f=1}^{N_f}\int_0^1dx_1\int_0^1dx_2\left[q_f(x_1,\mu)\bar{q}_f(x_2,\mu)+\bar{q}_f(x_1,\mu)q_f(x_2,\mu)\right] \\ &\times\hat{\sigma}_{S,V}^q(\hat{s},M_\Phi)\theta(\hat{s}-4M_\Phi^2), \end{aligned} \quad (40)$$

$$\sigma_{S,V}^{pp;g}(s,M_\Phi)=\int_0^1dx_1\int_0^1dx_2G(x_1,\mu)G(x_2,\mu)\hat{\sigma}_{S,V}^g(\hat{s},M_\Phi)\theta(\hat{s}-4M_\Phi^2). \quad (41)$$

$q_f(x,\mu)$ ,  $\bar{q}_f(x,\mu)$ , and  $G(x,\mu)$  denote the quark, antiquark and gluon distributions of the proton (antiproton), and  $\mu$  is the factorization scale.

## 4.2 $ep$ scattering

In  $ep$  scattering, the two contributions to the production cross section are the direct process  $\gamma^*g\rightarrow\Phi\bar{\Phi}$  [11] and the resolved photon process. Due to the photon-leptoquark coupling, the direct contribution,  $\sigma_{dir}$ , contains a factor  $Q_\Phi^2$  while the resolved one,  $\sigma_{res}$ , does not depend on the leptoquark charge. We use the Weizsäcker–Williams approximation (WWA) to describe the photon spectrum both in the case of the direct and resolved photon contributions. This approximation is known to hold at an accuracy of 10 to 15 %.

The total cross section is

$$\sigma_{S,V}^{ep,tot}=\sigma_{S,V}^{ep,dir}+\sigma_{S,V}^{ep,res}, \quad (42)$$

with (cf. [11])

$$\sigma_{S,V}^{ep,dir}=\int_{y_{min}}^{y_{max}}dy\int_{x_{min}}^{x_{max}}dx\phi_{\gamma/e}(y)G_p(x,\mu^2)\hat{\sigma}_{S,V}^{dir}(\hat{s},M_\Phi)\theta(\hat{s}-4M_\Phi^2), \quad (43)$$

where  $x_{min} = 4M_\Phi^2/yS$ ,  $\hat{s} = Sxy$ ,  $S = 4E_e E_p$ ,  $x_{max} = 1$ ,  $y = P.q/P.l_e$ , with  $q = l_e - l'_e$ , and  $P, l_e, l'_e$  the four momenta of the proton, the incoming and outgoing electron. The boundaries  $y_{min,max}$  are given by

$$y_{min,max} = \frac{S + \widetilde{W}^2 \pm \sqrt{(S - \widetilde{W}^2)^2 - 4m_e^2 \widetilde{W}^2}}{2(S + m_e^2)}, \quad (44)$$

where  $\widetilde{W}^2 = (2M_\Phi + m_p)^2 - m_p^2$ , and  $m_e$  and  $m_p$  are the electron and proton mass, respectively.  $\phi_{\gamma/e}(y)$  denotes the Weizsäcker-Williams distribution, see e.g. [30] :

$$\phi_{WWA}(y) = \frac{\alpha}{2\pi} \left[ 2m_e^2 y \left( \frac{1}{Q_{max}^2} - \frac{1}{Q_{min}^2} \right) + \frac{1 + (1-y)^2}{y} \log \frac{Q_{max}^2}{Q_{min}^2} \right]. \quad (45)$$

To parametrize the scales  $Q_{min,max}^2$  we choose the kinematic limits

$$Q_{min}^2 = \frac{m_e^2 y^2}{1-y}, \quad Q_{max}^2 = yS - 4M_\Phi^2 - 4M_\Phi m_p, \quad (46)$$

The cross sections in the  $\gamma^*g$  subsystem are

$$\hat{\sigma}_{S,V}^{dir}(\hat{s}, M_\Phi) = \frac{\pi\alpha\alpha_s(\mu^2)}{\hat{s}} Q_\Phi^2 R_{S,V}(\hat{s}, M_\Phi), \quad (47)$$

where

$$R_S = (2 - \beta^2)\beta - \frac{1}{2}(1 - \beta^4) \log \left| \frac{1 + \beta}{1 - \beta} \right|, \quad (48)$$

$$R_V = \sum_{j=0}^{20} \chi_j^*(\kappa_\gamma, \kappa_G, \lambda_\gamma, \lambda_G) \widetilde{H}_j(\hat{s}, \beta). \quad (49)$$

The functions  $\chi_j^*(\kappa_\gamma, \kappa_G, \lambda_\gamma, \lambda_G)$  and  $\widetilde{H}_j$  were given in ref. [11] in eqs. (12; A.2) where we defined  $\widetilde{H}_j \equiv (M_V^2/\hat{s}) \widetilde{F}_j^*$ <sup>9</sup>.

The cross sections due to the resolved photon contributions read:

$$\begin{aligned} \sigma_{S,V}^{ep,res}(s, M_\Phi) &= \int_{y_{min}}^{y_{max}} dy \int_{4M_\Phi^2/Sy}^1 dz \int_{4M_\Phi^2/Syz}^1 dx \phi_{\gamma/e}(y) \theta(\hat{s} - 4M_\Phi^2) \\ &\times \left\{ \sum_{f=1}^{N_f} \left[ q_f^\gamma(z, \mu_1) \bar{q}_f^p(x, \mu_2) + \bar{q}_f^\gamma(z, \mu_1) q_f^p(x, \mu_2) \right] \hat{\sigma}_{S,V}^q(\hat{s}, M_\Phi) \right. \\ &\left. + G^\gamma(z, \mu_1) G^p(x, \mu_2) \hat{\sigma}_{S,V}^g(\hat{s}, M_\Phi) \right\}. \quad (50) \end{aligned}$$

Here,  $q^{\gamma:p}$  and  $G^{\gamma:p}$  denote the quark and gluon densities in the photon and proton, respectively, and  $\hat{s} = xyzS$ .  $\mu_1$  and  $\mu_2$  are the mass factorization scales of the photon and proton distributions, which are different in general. The cross sections for the hadronic subprocesses  $\hat{\sigma}_{S,V}^{q,g}$  are given in eqs. (18,20,23,27).

<sup>9</sup> We have labeled the functions  $\chi_j$  and  $\widetilde{F}_j$  of [11] (A.2) by a star to distinguish them from those given in appendix B. The expression for  $\widetilde{F}^{18}$  in [11] contains a typographical error, the factor  $(1 - 6\beta^2)$  there should read  $(1 + 6\beta^2)$ .

### 4.3 $\gamma\gamma$ fusion

For  $\gamma\gamma$  or  $\gamma^*\gamma^*$  scattering three terms contribute to the cross section: the direct process  $\gamma\gamma \rightarrow \Phi\bar{\Phi}$ ,  $\sigma_{dir}$ , a term in which one of the photons is resolved and the second couples directly to the leptoquarks,  $\sigma_{dir/res}$ , and the double resolved contribution,  $\sigma_{res}$ ,

$$\sigma_{S,V}^{\gamma\gamma,tot} = \sigma_{S,V}^{\gamma\gamma,dir} + \sigma_{S,V}^{\gamma\gamma,dir/res} + \sigma_{S,V}^{\gamma\gamma,res}. \quad (51)$$

The third term (eq. (56)) is charge independent, but the first and the second terms behave  $\propto Q_\Phi^4$  and  $\propto Q_\Phi^2$ , respectively. The cross section for the direct contribution reads [13]

$$\sigma_{S,V}^{\gamma\gamma,dir}(s, M_\Phi) = \int_{y_{min}/y_{max}}^{y_{max}} dy_1 \int_{y_{min}/y_1}^{y_{max}} dy_2 \Phi_{\gamma/e}(y_1) \Phi_{\gamma/e}(y_2) \hat{\sigma}_{S,V}^{dir}(\hat{s}, M_\Phi) \theta(\hat{s} - 4M_\Phi^2). \quad (52)$$

Here the subsystem cross sections are:

$$\hat{\sigma}_{S,V}^{dir}(\hat{s}, M_\Phi) = \frac{\pi\alpha^2}{\hat{s}} Q_\Phi^4 N_c R_{S,V}^*(\hat{s}, M_\Phi), \quad (53)$$

with  $\hat{s} = y_1 y_2 S$ ,  $S = 4E_{e^+} E_{e^-}$ ,  $N_c = 3$ , and

$$\begin{aligned} R_S^* &= 2R_S, \\ R_V^* &= 2 \sum_{j=0}^{20} \chi_j^*(\kappa_\gamma, \kappa_\gamma, \lambda_\gamma, \lambda_\gamma) \widetilde{H}_j(\hat{s}, \beta). \end{aligned} \quad (54)$$

Effectively  $R_V^*$  depends on only 15 independent functions [13] due to the symmetry of the function  $\chi_j^*(\kappa_\gamma, \kappa_\gamma, \lambda_\gamma, \lambda_\gamma)$  in eq. (49).

The direct-resolved term is given by

$$\begin{aligned} \sigma_{S,V}^{\gamma\gamma,dir/res}(s, M_\Phi) &= 2 \int_{y_{min}/y_{max}}^{y_{max}} dy_1 \int_{y_{min}/y_1}^{y_{max}} dy_2 \int_{4M_\Phi^2/Sy_1y_2}^1 dz \Phi_{\gamma/e}(y_1) \Phi_{\gamma/e}(y_2) G_\gamma(z, \mu) \\ &\times \hat{\sigma}_{S,V}^{\gamma g}(\hat{s}, M_\Phi) \theta(\hat{s} - 4M_\Phi^2). \end{aligned} \quad (55)$$

with  $\mu$  the factorization scale. Because of the small size of the couplings  $\lambda_{lq} \ll e$  only the subprocess due to gluon-photon fusion contributes.

Finally the doubly-resolved contribution reads:

$$\begin{aligned} \sigma_{S,V}^{\gamma\gamma,res}(s, M_\Phi) &= \int_{y_{min}/y_{max}}^{y_{max}} dy_1 \int_{y_{min}/y_1}^{y_{max}} dy_2 \int_{4M_\Phi^2/Sy_1y_2}^1 dz_1 \int_{4M_\Phi^2/Sy_1y_2z_1}^1 dz_2 \Phi_{\gamma/e}(y_1) \Phi_{\gamma/e}(y_2) \\ &\times \left\{ \sum_{f=1}^{N_f} \left[ q_f^\gamma(z_1, \mu_1) \bar{q}_f^\gamma(z_2, \mu_2) + \bar{q}_f^\gamma(z_1, \mu_1) q_f^\gamma(z_2, \mu_2) \right] \hat{\sigma}_{S,V}^g(\hat{s}, M_\Phi) \right. \\ &\left. + G^\gamma(z_1, \mu_1) G^\gamma(z_2, \mu_2) \hat{\sigma}_{S,V}^g(\hat{s}, M_\Phi) \right\} \theta(\hat{s} - 4M_\Phi^2). \end{aligned} \quad (56)$$

where  $\hat{s} = y_1 y_2 z_1 z_2 S$ .

In  $e^+e^-$  scattering the functions  $\Phi_{\gamma/e}(y_i)$  denote the Weizsäcker-Williams distribution (45) with the parameters

$$Q_{i,min}^2 = \frac{m_e^2 y_i^2}{1 - y_i}, \quad Q_{i,max}^2 = Sy_i - 4M_\Phi^2 - 4M_\Phi m_e, \quad (57)$$

$$y_{min,max} = \frac{S + \widetilde{W}^{*2} \pm \sqrt{(S - \widetilde{W}^{*2})^2 - 4m_e^2 \widetilde{W}^{*2}}}{2(S + m_e^2)}, \quad (58)$$

and  $W^{*2} = (m_e + 2M_\Phi)^2 - m_e^2$ .

For a  $\gamma\gamma$  collider operating with photon beams which are produced by laser back scattering, the spectrum  $\Phi_{\gamma/e}(y)$  is given by

$$\phi_C(y) = \frac{1}{N(x)} \left[ 1 - y + \frac{1}{1-y} - \frac{4y}{x(1-y)} + \frac{4y^2}{x^2(1-y)^2} \right], \quad (59)$$

with

$$N(x) = \frac{16 + 32x + 18x^2 + x^3}{2x(1+x)^2} + \frac{x^2 - 4x - 8}{x^2} \ln(1+x), \quad (60)$$

and

$$0 = y_{min} \leq y \leq y_{max} = x/(x+1), \quad x = 2(\sqrt{2} + 1), \quad (61)$$

cf. [31]. Here complete beam conversion is assumed for the laser back scattering process. We use eq. (59) as an approximate description, which may be needed to be refined according to different technical aspects at future  $\gamma\gamma$  colliders [32].

## 5 Numerical Results

### 5.1 $p\bar{p}$ and $pp$ scattering

The different numerical values of the cross sections for leptoquark pair production at  $p\bar{p}$  and  $pp$  colliders calculated below are determined by the different resulting parton-parton luminosities  $\tau d\mathcal{L}/d\tau$ . In the collinear picture described above, the differential luminosities are

$$\tau \frac{d\mathcal{L}^q}{d\tau} = \tau \int_\tau^1 \frac{dx}{x} \sum_{i=1}^{N_f} \left[ f_{q_i/a}(x, \mu_1) f_{\bar{q}_i/b}\left(\frac{\tau}{x}, \mu_2\right) + f_{\bar{q}_i/a}(x, \mu_1) f_{q_i/b}\left(\frac{\tau}{x}, \mu_2\right) \right], \quad (62)$$

$$\tau \frac{d\mathcal{L}^g}{d\tau} = \tau \int_\tau^1 \frac{dx}{x} f_{g/a}(x, \mu_1) f_{g/b}\left(\frac{\tau}{x}, \mu_2\right), \quad (63)$$

with  $\tau = \hat{s}/s$ , and  $\mu_1$  and  $\mu_2$  are the corresponding factorization scales. In figure 3 a comparison of the quark-antiquark and gluon-gluon luminosities is given for the kinematic range at the TEVATRON and LHC. We used the distributions [33]<sup>10</sup> to describe the parton densities of the proton and choose  $\mu_1 = \mu_2 = \sqrt{\hat{s}} \equiv \sqrt{\tau s}$  in the following.

At a fixed value of  $\tau$  the differential quark-antiquark luminosity  $\tau(d\mathcal{L}^q/d\tau)$  at the TEVATRON is much larger than at LHC. The corresponding values for  $\tau(d\mathcal{L}^g/d\tau)$  are rather similar. Since the dominant contributions to the scattering cross sections at LHC are due to lower  $\tau$  values when compared to the range at the TEVATRON, large contributions to the scattering cross section are expected for the gluon fusion process. On the other hand, the quark-antiquark annihilation process is expected to yield a large contribution to the scattering cross section at the TEVATRON.

In figures 4a,b, the pair production cross sections for scalar leptoquarks at the TEVATRON and LHC are shown for the mass range  $M_S \geq 100$  GeV. The respective contributions to the cross section due to quark-antiquark and gluon-gluon scattering are basically a consequence of

<sup>10</sup>Other parametrizations of the parton densities in the proton [34] agree very well with the parametrization [33].

the behaviour of the differential parton luminosities: whereas the quark terms yield the largest contributions to the cross section at the TEVATRON in this mass range, at LHC the dominant contribution is due to gluon-gluon fusion. The quark contributions become important also at LHC energies for large masses.

The production cross sections for vector leptoquarks at the TEVATRON and LHC are shown in figures 5a,b. We observe a sizeable dependence of the cross section on the value of both the anomalous couplings  $\kappa_G$  and  $\lambda_G$ . Moreover, their impact on the quark and gluon contributions turns out to be different. As in the case of scalar leptoquarks the production cross section at the TEVATRON, figure 5a, is dominated by the quark contributions. On the other hand the gluonic terms dominate in the case of LHC, figure 5b. The numerical values of the cross sections agree with those calculated in [35] (fig. 18,19), [36]<sup>11</sup>, for selected values of  $\kappa_G = 1, 0$  and  $\lambda_G \equiv 0$  treated there, within the uncertainty due to the different parton densities used.

We vary both  $\kappa_G$  and  $\lambda_G$  to illustrate the overall behaviour and consider all combinations  $\kappa_G, \lambda_G$  at a fixed, characteristic leptoquark mass. These variations lead to changes of about two orders of magnitude in the production cross sections both at LHC and the TEVATRON allowing for  $-0.5 \leq \kappa_G < 3.5$  and  $\lambda_G < 1$ . In figure 6a,b the dependence of the total production cross section is shown for the case of the TEVATRON and LHC, assuming  $M_{LQ} = 150$  GeV and  $M_{LQ} = 500$  GeV, respectively. In neither case is the minimal cross section obtained for anomalous couplings close to the Yang-Mills type couplings. For TEVATRON energies the minimal cross section is obtained for  $\lambda_G = -0.208, \kappa_G = 1.3$  choosing  $M_V = 150$  GeV as an example. On the other hand, at LHC for  $M_V = 500$  GeV the minimal cross section is obtained for  $\lambda_G = -0.052, \kappa_G = 1.02$ . The latter values are rather close to those in the case of a minimal vector coupling.

For the determination of the leptoquark signal both the rapidity and  $p_\perp$  distributions may be used. They are shown in figures 7 and 8 for the kinematic ranges at the TEVATRON and LHC assuming the above leptoquark masses as examples. The rapidity distributions for both scalar and vector leptoquark pair production are wider at LHC compared to those at the TEVATRON, which are more peaked at  $|\eta| \sim 0$ . The  $p_\perp$  distribution for scalar and vector leptoquarks at the TEVATRON (figures 8 a,b) peak at  $p_\perp \sim 100$  GeV, while the corresponding  $p_\perp$  distributions at LHC are much wider and peak positions of  $p_\perp \sim 150$  GeV for scalar and  $p_\perp \sim 300$  GeV for vector leptoquarks with a minimal vector coupling are found.

The estimates given are illustrative and can not replace a complete analysis which accounts for specific experimental and detector details in the respective experiments and a detailed investigation of background reactions. This is not the intention of the present paper. The numbers given below for accessible mass ranges (section 5.4) are therefore meant to be indicative since they are based on the signal events only. They serve as an illustration of the principal search potential in different reactions and at different colliders.

## 5.2 $ep$ scattering

Figure 9a shows the dependence of the integrated production cross section on the leptoquark mass for scalar pair production at HERA for both  $|Q_\Phi| = 5/3$  and  $1/3$ . For the calculation of the resolved photon contribution we used the parametrization [38] to describe the parton densities of the photon. The mass dependence of the cross sections in the range  $M_\Phi > 40$  GeV is found to be nearly exponential. For low charge leptoquarks the resolved photon terms dominate, whereas for leptoquarks with a high charge the largest contribution to the cross section is due to the direct

<sup>11</sup>A recent numerical update was given in ref. [37].

term. A similar behaviour is observed in a more extended mass range for the same process at LEP  $\otimes$  LHC, see figure 9b.

For the case of vector leptoquark pair production we consider different choices of the anomalous couplings in the range  $\kappa, \lambda \in [-1, +1]$ , and put  $\kappa_\gamma = \kappa_G$  and  $\lambda_\gamma = \lambda_G$  always.

For the kinematic range of HERA figure 10a shows the cross sections for vector leptoquark pair production for a selection of anomalous couplings. Rather large cross sections are obtained for the choice  $\kappa_{\gamma,G} = \lambda_{\gamma,G} = -1$ . The pair production cross sections are larger in the case of Yang-Mills type gauge boson-leptoquark couplings  $\kappa_{\gamma,G} = \lambda_{\gamma,G} = 0$  than in the case of minimal couplings  $\kappa_{\gamma,G} = 1, \lambda_{\gamma,G} = 0$ . Although the accessible mass range at HERA is smaller than that at the TEVATRON, a search for vector leptoquark pair production at HERA for third generation leptoquarks appears to be worthwhile, cf. [8]. In  $ep$  scattering, besides the anomalous couplings of the gluon also those of the photon are probed and corresponding constraints can be derived.

An analogous behaviour of the scattering cross sections, covering a wider mass range, is obtained for the same processes at LEP  $\otimes$  LHC, see figure 10b.

### 5.3 $\gamma\gamma$ scattering

The different contributions to the integrated pair production cross section for scalar leptoquarks at a future  $e^+e^-$  linear collider operating at  $\sqrt{s} = 500$  GeV are depicted in figure 11a. For leptoquarks carrying a charge  $|Q_\Phi| = 5/3$  the direct process in the reaction  $e^+e^- \rightarrow \Phi\bar{\Phi}X$ <sup>12</sup> dominates at lower values of  $\beta$ . Here the virtual photon spectra were approximated by the Weizsäcker–Williams distribution, eq. (45). At large  $\beta$  the cross section is further enhanced by the resolved photon contributions. On the other hand, for low charge leptoquarks as  $|Q_\Phi| = 1/3$ , the direct contribution is suppressed by orders of magnitude against the resolved photon terms.

In figure 11b the contributions to the production cross sections are shown for scalar leptoquarks at a  $\gamma\gamma$  collider at  $\sqrt{s} = 500$  GeV. The general observation is the same as in the previous case but at lower values of  $\beta$  larger cross sections are obtained. For leptoquarks of a charge  $|Q_\Phi| = 5/3$  thus nearly the complete accessible phase space can be probed.

As in the case of  $ep$  scattering we consider a series of anomalous couplings for vector leptoquark pair production. Numerical results are illustrated for the process  $\gamma^*\gamma^* \rightarrow V\bar{V}$  at an  $e^+e^-$  linear collider at  $\sqrt{s} = 500$  GeV assuming Weizsäcker-Williams spectra for the virtual photons, in figure 12a. Among the different choices of anomalous couplings considered, the smallest cross sections were obtained for the minimal vector couplings. The corresponding cases for a  $\gamma\gamma$  collider operating at the same cms energy are depicted in figure 12b. For all three choices of the anomalous couplings, the accessible search range reaches nearly the kinematic boundary for  $|Q_\Phi| = 5/3$  leptoquarks, while for  $|Q_\Phi| = 1/3$  leptoquarks the corresponding limits are smaller.

### 5.4 A comparison of the search potential at different colliders

The leptoquark search limits which can be reached for the reactions discussed in the previous sections at different high energy colliders are summarized in table 2. Estimates of the accessible mass ranges are given based on 10 and 100 signal events, respectively. Here we consider the mass range above 45 GeV, which was already widely excluded by the searches at LEP 1, cf. [4].

<sup>12</sup> Here we do not consider the contributions of the process  $e^+e^- \rightarrow \Phi\bar{\Phi}$  which was dealt with in ref. [15] previously. For a detailed investigation of this process for the case of vector leptoquarks with general anomalous couplings  $\kappa_{\gamma,Z}, \lambda_{\gamma,Z}$ , see ref. [39].

For hadron colliders such as the TEVATRON and LHC the search limits are flavor and family independent. Since in the other reactions also photon-leptoquark interactions contribute<sup>13</sup>, the respective event rates depend partly on the leptoquark charge.

Collider	Mode	$\sqrt{S}$	Luminosity	Q	Scalar Leptoquarks		Vector Leptoquarks	
					100#	10#	100#	10#
TEVATRON	$p\bar{p}$	1.8 TeV	$100pb^{-1}$		140	200	170	225
TEV33	$p\bar{p}$	2.0 TeV	$1fb^{-1}$		210	290	290	370
LHC	$pp$	14 TeV	$10fb^{-1}$		900	1200	1200	1500
HERA	$ep$	314 GeV	$100pb^{-1}$	1/3	-	50	50	60
				5/3	45	60	60	75
				1/3	45	60	60	75
				5/3	55	75	70	85
LEP $\otimes$ LHC	$ep$	1.26 TeV	$1fb^{-1}$	1/3	125	180	180	240
				5/3	165	225	210	270
LINAC $e^+e^-$	$\gamma^*\gamma^*$ WWA	500 GeV	$10fb^{-1}$	1/3	90	120	120	155
				5/3	135	185	170	210
LINAC $e^+e^-$	$\gamma\gamma$ Compton	500 GeV	$10fb^{-1}$	1/3	160	180	175	190
				5/3	200	205	200	205
LINAC $e^+e^-$	$\gamma^*\gamma^*$ WWA	1 TeV	$10fb^{-1}$	1/3	140	195	285	345
				5/3	220	325	435	470
LINAC $e^+e^-$	$\gamma\gamma$ Compton	1 TeV	$10fb^{-1}$	1/3	300	340	390	405
				5/3	400	405	410	410

Table 2: Accessible mass ranges for leptoquark pair production (GeV) for  $M_{S,V} \geq 45$  GeV. For the case of vector leptoquarks the mass ranges correspond to  $\kappa_G = 1.3$ ,  $\lambda_G = -0.21$  at the TEVATRON, and the minimum vector coupling  $\kappa_G = 1$ ,  $\lambda_G = 0$  for all other cases.

In the foreseeable future, the widest mass range can be explored at LHC reaching masses of  $O(1$  to  $1.5$  TeV) at  $\mathcal{L} = 10 fb^{-1}$ . The accessible mass ranges at future  $\gamma\gamma$  colliders operating at  $\sqrt{s} = 1$  TeV, using laser back scattering to form the photon beams, reach masses of  $O(400$  GeV) at the same integrated luminosity. For comparison, the mass range of  $O(200$  GeV) and  $O(450$  GeV), respectively, can be reached for the case of all scalar and vector leptoquarks discussed in [16] for the pair production process  $e^+e^- \rightarrow \Phi\bar{\Phi}$  at  $\sqrt{s} = 1$  TeV at an integrated luminosity of  $\mathcal{L} = 10 fb^{-1}$ , assuming the minimal coupling for the vector states, cf. [15]. The mass ranges of  $O(200$  GeV) are accessible at  $e^+e^-$  linear colliders with a cms energy of  $\sqrt{s} = 500$  GeV, a possible future  $ep$  collider at LEP $\otimes$ LHC, and at the TEVATRON. One should note, however, that the different scattering processes at  $pp$ ,  $p\bar{p}$ ,  $ep$ ,  $e^+e^-$ , and  $\gamma\gamma$  colliders are not suited to limit all the specific production channels equally well. Particularly the search for third generation leptoquarks is difficult at hadron colliders [8]. Though the accessible mass ranges for LEP 2 [15, 39] and HERA are bounded to 90 GeV and below, depending on the respective leptoquark type, at both colliders one may search for these particles.

<sup>13</sup>Additional contributions due to Higgs-, Z- and  $W^\pm$ -boson couplings are not considered in the present paper.

## 6 Conclusions

The differential and integral hadronic pair production cross sections for scalar and vector leptoquarks were calculated. In the latter case, we accounted for general anomalous couplings,  $\kappa_G$  and  $\lambda_G$ . Predictions were made on the discovery potential of leptoquarks at present and future high energy colliders. The processes considered set mass bounds in a widely model independent way since the scattering cross sections depend on the known gauge couplings. In the case of vector leptoquarks in the mass range  $M_V \lesssim 1$  TeV, anomalous couplings also emerge since these particles are not gauge bosons. However, as was shown explicitly for the case of  $p\bar{p}$  and  $pp$  scattering, a set of anomalous couplings  $\kappa_G^{min}, \lambda_G^{min}$  exists yielding a non-zero, minimal production cross section. Due to this global mass bounds may be derived.

Hadron colliders cover the widest mass range for leptoquark searches based on pair production. Therefore the best constraints are expected from the TEVATRON in the near future, and later from LHC for those signatures which can be well separated from the background at these colliders. It appears to be likely that one may search for first and second generation leptoquarks in this way in the mass range up to 1.2 and 1.5 TeV for the expected scalar and vector states.

A more difficult case concerns the 3rd generation leptoquarks decaying into  $\tau b$ , e.g. This type of signature may be more easily isolated at colliders with a lower hadronic background. As evident from the explorable mass ranges, leptoquark searches may be carried out looking for those spectacular decay channels as  $\Phi \rightarrow t\tau$  at LHC and future linear colliders.

**Acknowledgments:** We would like to thank Prof. P. Söding for his constant support of the present project. Our thanks are due to A. Pukhov for the help through the implementation of the interaction Lagrangian (2) into **CompHEP**, and both A. Pukhov and V. Ilyin for discussions. We would like to thank S. Riemersma for a careful reading of the manuscript. E.B. and A.K. would like to thank DESY–Zeuthen for the warm hospitality extended to them. The work has been supported in part by the EC grant ‘Capital Humain et Mobilite’ CHRX–CT92–0004, by the grant 95-0-6.4-38 of the Center of Natural Sciences of the State Committee for Higher Education in Russia, and by the RFBR grants 96-02-18635a and 96-02-19773a.



# A Feynman Rules

We use the convention of ref. [40]. All momenta are incoming. The propagators of the gluon-, ghost-, fermion-, and leptoquark fields are:

$$D_{\mu\nu}^{ab,g}(k) = \delta^{ab} d^{\mu\nu}(k) \frac{1}{k^2}, \quad (64)$$

$$\hat{\Delta}^{ab,\hat{g}}(k) = -\delta^{ab} \frac{1}{k^2}, \quad (65)$$

$$G_{ij}(p) = \delta_{ij} \frac{1}{m_q - \not{p}}, \quad (66)$$

$$D_{ab}^S(k) = -\delta_{ab} \frac{1}{k^2 - M_S^2}, \quad (67)$$

$$D_{ab}^{\mu\nu,V}(k) = \delta_{ab} \Delta^{\mu\nu}(k) \frac{1}{k^2 - M_V^2}, \quad (68)$$

with

$$d_{\mu\nu}(k) = g_{\mu\nu} - (1 - \xi) \frac{k_\mu k_\nu}{k^2}, \quad (69)$$

$$\Delta_{\mu\nu}(k) = g_{\mu\nu} - \frac{k_\mu k_\nu}{M_V^2}. \quad (70)$$

$\xi$  denotes the gauge parameter of the gluon field in  $R_\xi$  gauges.

The triple vertices are:

$$V_{\mu_1\mu_2\mu_3}^{ggg,a_1a_2a_3} = -i f^{abc} g_s \hat{V}_{\mu_1\mu_2\mu_3}(k_1, k_2, k_3), \quad (71)$$

$$V_{\mu}^{\hat{g}\hat{g}g,a_1a_2a_3} = -i g_s f^{abc} k_{2\mu}, \quad (72)$$

$$V_{\mu}^{qqg,ija} = g_s \gamma_{\mu} t_{ij}^a, \quad (73)$$

$$V_{\mu_3}^{\bar{S}Sg,aij}(k_1, k_2, k_3) = g_s (t^a)^{ij} (k_2 - k_1)_{\mu_3}, \quad (74)$$

$$V_{\mu_1\mu_2\mu_3}^{\bar{V}Vg,aij}(k_1, k_2, k_3) = g_s (t^a)^{ij} \left[ \hat{V}_{\mu_1\mu_2\mu_3} + \kappa_G \hat{V}_{\mu_1\mu_2\mu_3}^{\kappa} + \frac{\lambda_G}{M_V^2} \hat{V}_{\mu_1\mu_2\mu_3}^{\lambda} \right], \quad (75)$$

where

$$\hat{V}_{\mu_1,\mu_2,\mu_3}(k_1, k_2, k_3) = (k_1 - k_2)_{\mu_3} g_{\mu_1\mu_2} + (k_2 - k_3)_{\mu_1} g_{\mu_2\mu_3} + (k_3 - k_1)_{\mu_2} g_{\mu_3\mu_1}, \quad (76)$$

$$\hat{V}_{\mu_1\mu_2\mu_3}^{\kappa}(k_1, k_2, k_3) = k_{3\mu_1} g_{\mu_2\mu_3} - k_{3\mu_2} g_{\mu_1\mu_3}, \quad (77)$$

$$\begin{aligned} \hat{V}_{\mu_1\mu_2\mu_3}^{\lambda}(k_1, k_2, k_3) &= (k_1 \cdot k_2) (k_{3\mu_1} g_{\mu_2\mu_3} - k_{3\mu_2} g_{\mu_1\mu_3}) + (k_2 \cdot k_3) (k_{1\mu_2} g_{\mu_1\mu_3} - k_{1\mu_3} g_{\mu_1\mu_2}) \\ &+ (k_3 \cdot k_1) (k_{2\mu_3} g_{\mu_1\mu_2} - k_{2\mu_1} g_{\mu_2\mu_3}) + k_{1\mu_3} k_{2\mu_1} k_{3\mu_2} - k_{1\mu_2} k_{2\mu_3} k_{3\mu_1}. \end{aligned} \quad (78)$$

The four-vertices are:

$$\begin{aligned} W_{\mu_1\mu_2\mu_3\mu_4}^{gggg,a_1a_2a_3a_4}(k_1, k_2, k_3, k_4) &= -g_s^2 \left\{ f^{a_1a_2b} f^{a_3a_4b} (g_{\mu_1\mu_3} g_{\mu_2\mu_4} - g_{\mu_1\mu_4} g_{\mu_2\mu_3}) \right. \\ &+ f^{a_1a_3b} f^{a_2a_4b} (g_{\mu_1\mu_2} g_{\mu_3\mu_4} - g_{\mu_1\mu_4} g_{\mu_2\mu_3}) \\ &\left. + f^{a_1a_4b} f^{a_3a_2b} (g_{\mu_1\mu_3} g_{\mu_2\mu_4} - g_{\mu_1\mu_2} g_{\mu_3\mu_4}) \right\}, \end{aligned} \quad (79)$$

$$W_{\mu_1\mu_2}^{\bar{S}Sgg,ija_1a_2}(p_1, p_2, p_3, p_4) = g_s^2 (t^{a_1} t^{a_2} + t^{a_2} t^{a_1})^{ij} g_{\mu_1\mu_2}, \quad (80)$$

$$\begin{aligned}
W_{\mu_1\mu_2\mu_3\mu_4}^{\overline{V}Vgg,ij a_1 a_2}(p_1, p_2, p_3, p_4) &= -g_s^2 \left\{ (t^{a_1} t^{a_2})^{ij} \left[ \widehat{W}_{\mu_1\mu_2\mu_3\mu_4} + \kappa_G \widehat{W}_{\mu_1\mu_2\mu_3\mu_4}^\kappa + \frac{\lambda_G}{M_V^2} \widehat{W}_{\mu_1\mu_2\mu_3\mu_4}^\lambda \right] \right. \\
&\quad \left. + (t^{a_2} t^{a_1})^{ij} \left[ \widehat{W}_{\mu_1\mu_2\mu_4\mu_3} + \kappa_G \widehat{W}_{\mu_1\mu_2\mu_4\mu_3}^\kappa + \frac{\lambda_G}{M_V^2} \widehat{W}_{\mu_1\mu_2\mu_4\mu_3}^\lambda \right] \right\}, \quad (81)
\end{aligned}$$

with

$$\widehat{W}_{\mu_1\mu_2\mu_3\mu_4}(p_1, p_2, p_3, p_4) = g_{\mu_1\mu_2} g_{\mu_3\mu_4} + g_{\mu_1\mu_3} g_{\mu_2\mu_4} - 2g_{\mu_1\mu_4} g_{\mu_2\mu_3}, \quad (82)$$

$$\widehat{W}_{\mu_1\mu_2\mu_3\mu_4}^\kappa(p_1, p_2, p_3, p_4) = g_{\mu_1\mu_4} g_{\mu_2\mu_3} - g_{\mu_1\mu_3} g_{\mu_2\mu_4}, \quad (83)$$

$$\begin{aligned}
\widehat{W}_{\mu_1\mu_2\mu_3\mu_4}^\lambda(p_1, p_2, p_3, p_4) &= (p_1 \cdot p_2)(g_{\mu_1\mu_4} g_{\mu_2\mu_3} - g_{\mu_1\mu_3} g_{\mu_2\mu_4}), \\
&\quad + (p_1 \cdot p_3)(g_{\mu_1\mu_4} g_{\mu_2\mu_3} - g_{\mu_1\mu_2} g_{\mu_3\mu_4}) \\
&\quad + (p_2 \cdot p_4)(g_{\mu_1\mu_4} g_{\mu_2\mu_3} - g_{\mu_1\mu_2} g_{\mu_3\mu_4}) \\
&\quad + g_{\mu_1\mu_2}(p_{1\mu_3} p_{3\mu_4} + p_{2\mu_4} p_{4\mu_3} + p_{1\mu_4} p_{2\mu_3} - p_{1\mu_3} p_{2\mu_4}) \\
&\quad + g_{\mu_1\mu_3}(p_{1\mu_2} p_{2\mu_4} + p_{1\mu_4} p_{3\mu_2} - p_{1\mu_2} p_{3\mu_4}) \\
&\quad - g_{\mu_1\mu_4}(p_{1\mu_2} p_{2\mu_3} + p_{1\mu_3} p_{3\mu_2} + p_{2\mu_3} p_{4\mu_2}) \\
&\quad - g_{\mu_2\mu_3}(p_{2\mu_1} p_{1\mu_4} + p_{2\mu_4} p_{4\mu_1} + p_{1\mu_4} p_{3\mu_1}) \\
&\quad + g_{\mu_2\mu_4}(p_{2\mu_1} p_{1\mu_3} + p_{2\mu_3} p_{4\mu_1} - p_{2\mu_1} p_{4\mu_3}) \\
&\quad + g_{\mu_3\mu_4}(p_{1\mu_2} p_{3\mu_1} + p_{2\mu_1} p_{4\mu_2}). \quad (84)
\end{aligned}$$

## B Coefficients of the production cross section of vector leptoquarks

The functions  $F_i(\hat{s}, \beta, \cos \theta)$  which determine the differential pair production cross section for  $gg \rightarrow V\bar{V}$  are:

$$F_0 = \left[ 19 - 6\beta^2 + 6\beta^4 + (16 - 6\beta^2) \beta^2 \cos^2 \theta + 3\beta^4 \cos^4 \theta \right] \cdot (7 + 9\beta^2 \cos^2 \theta) \quad (85)$$

$$F_1 = -4 \cdot (77 + 143\beta^2 \cos^2 \theta + 36\beta^4 \cos^4 \theta) \quad (86)$$

$$F_2 = -8 \cdot (7 + 11\beta^2 \cos^2 \theta - 18\beta^4 \cos^4 \theta) \quad (87)$$

$$F_3 = 2 \cdot (117 + 185\beta^2 \cos^2 \theta + 18\beta^4 \cos^4 \theta) + 2 \frac{\hat{s}}{M_\Phi^2} (8 - \beta^2 \cos^2 \theta - 7\beta^4 \cos^4 \theta) \\ + \frac{7}{4} \frac{\hat{s}^2}{M_\Phi^4} (1 - \beta^2 \cos^2 \theta)^2 \quad (88)$$

$$F_4 = -4 \cdot (19 + 27\beta^2 \cos^2 \theta + 18\beta^4 \cos^4 \theta) + 10 \frac{\hat{s}}{M_\Phi^2} (1 - \beta^2 \cos^2 \theta) (7 - \beta^2 \cos^2 \theta) \quad (89)$$

$$F_5 = 2 \cdot (19 + 27\beta^2 \cos^2 \theta + 18\beta^4 \cos^4 \theta) - \frac{\hat{s}}{M_\Phi^2} (1 - \beta^2 \cos^2 \theta) (65 + 29\beta^2 \cos^2 \theta) \\ + \frac{1}{8} \frac{\hat{s}^2}{M_\Phi^4} (1 - \beta^2 \cos^2 \theta) (97 + 2\beta^2 \cos^2 \theta - 115\beta^4 \cos^4 \theta) + \frac{\hat{s}^3}{M_\Phi^6} \frac{9}{4} (1 - \beta^2 \cos^2 \theta)^3 \quad (90)$$

$$F_6 = -61 - 67\beta^2 \cos^2 \theta - \frac{1}{2} \frac{\hat{s}}{M_\Phi^2} (1 - \beta^2 \cos^2 \theta) (39 + 14\beta^2 \cos^2 \theta) \\ - \frac{7}{4} \frac{\hat{s}^2}{M_\Phi^4} (1 - \beta^2 \cos^2 \theta)^2 \quad (91)$$

$$F_7 = 127 + 129\beta^2 \cos^2 \theta - \frac{1}{2} \frac{\hat{s}}{M_\Phi^2} (1 - \beta^2 \cos^2 \theta) (89 + 3\beta^2 \cos^2 \theta) \\ + \frac{1}{4} \frac{\hat{s}^2}{M_\Phi^4} (1 - \beta^2 \cos^2 \theta)^2 (-23 + 18\beta^2 \cos^2 \theta) \quad (92)$$

$$F_8 = -71 - 57\beta^2 \cos^2 \theta + \frac{1}{2} \frac{\hat{s}}{M_\Phi^2} (1 - \beta^2 \cos^2 \theta) (170 + 21\beta^2 \cos^2 \theta) \\ + \frac{1}{4} \frac{\hat{s}^2}{M_\Phi^4} (1 - \beta^2 \cos^2 \theta) (-59 + 40\beta^2 \cos^2 \theta + 27\beta^4 \cos^4 \theta) - \frac{9}{4} \frac{\hat{s}^3}{M_\Phi^6} (1 - \beta^2 \cos^2 \theta)^3 \quad (93)$$

$$F_9 = 5 (1 - \beta^2 \cos^2 \theta) - \frac{\hat{s}}{M_\Phi^2} (1 - \beta^2 \cos^2 \theta) (21 + 2\beta^2 \cos^2 \theta) \\ + \frac{1}{4} \frac{\hat{s}^2}{M_\Phi^4} (1 - \beta^2 \cos^2 \theta)^2 (74 + 9\beta^2 \cos^2 \theta) \\ + \frac{1}{4} \frac{\hat{s}^3}{M_\Phi^6} (1 - \beta^2 \cos^2 \theta)^2 (-15 + 8\beta^2 \cos^2 \theta) \quad (94)$$

$$F_{10} = 3 + 5\beta^2 \cos^2 \theta + \frac{5}{4} \frac{\hat{s}}{M_\Phi^2} (1 - \beta^2 \cos^2 \theta) (4 - \beta^2 \cos^2 \theta) \\ + \frac{1}{32} \frac{\hat{s}^2}{M_\Phi^4} (1 - \beta^2 \cos^2 \theta)^2 (25 + 13\beta^2 \cos^2 \theta) \quad (95)$$

$$\begin{aligned}
F_{11} &= -4 \cdot (3 + 5\beta^2 \cos^2 \theta) - 5 \frac{\hat{s}}{M_\Phi^2} (1 - \beta^2 \cos^2 \theta)^2 \\
&+ \frac{1}{8} \frac{\hat{s}^2}{M_\Phi^4} (1 - \beta^2 \cos^2 \theta)^2 (35 - 13\beta^2 \cos^2 \theta)
\end{aligned} \tag{96}$$

$$\begin{aligned}
F_{12} &= 6 \cdot (3 + 5\beta^2 \cos^2 \theta) - \frac{15}{2} \frac{\hat{s}}{M_\Phi^2} (1 - \beta^2 \cos^2 \theta) (2 + \beta^2 \cos^2 \theta) \\
&+ \frac{1}{16} \frac{\hat{s}^2}{M_\Phi^4} (1 - \beta^2 \cos^2 \theta) (-23 + 54\beta^2 \cos^2 \theta - 39\beta^4 \cos^4 \theta) \\
&+ \frac{1}{64} \frac{\hat{s}^3}{M_\Phi^6} (1 - \beta^2 \cos^2 \theta)^2 (113 - 49\beta^2 \cos^2 \theta)
\end{aligned} \tag{97}$$

$$\begin{aligned}
F_{13} &= -4 \cdot (3 + 5\beta^2 \cos^2 \theta) + 5 \frac{\hat{s}}{M_\Phi^2} (1 - \beta^2 \cos^2 \theta) (5 + \beta^2 \cos^2 \theta) \\
&- \frac{1}{8} \frac{\hat{s}^2}{M_\Phi^4} (1 - \beta^2 \cos^2 \theta)^2 (119 + 13\beta^2 \cos^2 \theta) \\
&+ \frac{1}{32} \frac{\hat{s}^3}{M_\Phi^6} (1 - \beta^2 \cos^2 \theta)^2 (79 - 15\beta^2 \cos^2 \theta)
\end{aligned} \tag{98}$$

$$\begin{aligned}
F_{14} &= 3 + 5\beta^2 \cos^2 \theta - \frac{5}{4} \frac{\hat{s}}{M_\Phi^2} (1 - \beta^2 \cos^2 \theta) (8 + \beta^2 \cos^2 \theta) \\
&+ \frac{1}{32} \frac{\hat{s}^2}{M_\Phi^4} (1 - \beta^2 \cos^2 \theta) (321 - 324\beta^2 \cos^2 \theta - 13\beta^4 \cos^4 \theta) \\
&+ \frac{11}{64} \frac{\hat{s}^3}{M_\Phi^6} (1 - \beta^2 \cos^2 \theta)^2 (-23 + 7\beta^2 \cos^2 \theta) \\
&+ \frac{1}{256} \frac{\hat{s}^4}{M_\Phi^8} (1 - \beta^2 \cos^2 \theta)^2 (135 - 22\beta^2 \cos^2 \theta + 15\beta^4 \cos^4 \theta).
\end{aligned} \tag{99}$$

The coefficients  $\tilde{F}_i(\hat{s}, \beta)$  for the integrated cross section for  $gg \rightarrow V\bar{V}$  are:

$$\tilde{F}_0 = \beta \left( \frac{523}{4} - 90\beta^2 + \frac{93}{4}\beta^4 \right) - \frac{3}{4} (65 - 83\beta^2 + 19\beta^4 - \beta^6) \log \left| \frac{1+\beta}{1-\beta} \right|$$

$$\tilde{F}_1 = -4\beta(41 - 9\beta^2) - \frac{87}{2}(1 - \beta^2) \log \left| \frac{1+\beta}{1-\beta} \right| \tag{100}$$

$$\tilde{F}_2 = 36\beta(1 - \beta^2) - 25(1 - \beta^2) \log \left| \frac{1+\beta}{1-\beta} \right| \tag{101}$$

$$\tilde{F}_3 = \beta(75 - 9\beta^2) + \frac{7}{4}\beta \frac{\hat{s}}{M_\Phi^2} - \frac{1}{4}(1 - 61\beta^2) \log \left| \frac{1+\beta}{1-\beta} \right| \tag{102}$$

$$\tilde{F}_4 = -2\beta(20 - 9\beta^2) + \frac{1}{2}(91 - 31\beta^2) \log \left| \frac{1+\beta}{1-\beta} \right| \tag{103}$$

$$\tilde{F}_5 = \beta \left( \frac{209}{6} - 9\beta^2 \right) + \frac{263}{12}\beta \frac{\hat{s}}{M_\Phi^2} + \frac{3}{2}\beta \frac{\hat{s}^2}{M_\Phi^4} - \left( \frac{219}{4} - \frac{31}{4}\beta^2 + \frac{\hat{s}}{M_\Phi^2} \right) \log \left| \frac{1+\beta}{1-\beta} \right| \tag{104}$$

$$\tilde{F}_6 = -9\beta - \frac{7}{4}\beta \frac{\hat{s}}{M_\Phi^2} - \left( \frac{103}{8} + \frac{3}{8}\beta^2 \right) \log \left| \frac{1+\beta}{1-\beta} \right| \tag{105}$$

$$\tilde{F}_7 = \frac{55}{2}\beta - \frac{17}{4}\beta \frac{\hat{s}}{M_\Phi^2} - \left( \frac{185}{8} - \frac{1}{8}\beta^2 \right) \log \left| \frac{1+\beta}{1-\beta} \right| \tag{106}$$

$$\tilde{F}_8 = -\frac{35}{2}\beta - 22\beta\frac{\hat{s}}{M_\Phi^2} - \frac{3}{2}\beta\frac{\hat{s}^2}{M_\Phi^4} + \left(\frac{375}{8} + \frac{7}{8}\beta^2 + \frac{\hat{s}}{M_\Phi^2}\right) \log\left|\frac{1+\beta}{1-\beta}\right| \quad (107)$$

$$\tilde{F}_9 = -\beta + \frac{199}{12}\beta\frac{\hat{s}}{M_\Phi^2} - \frac{37}{12}\beta\frac{\hat{s}^2}{M_\Phi^4} - \left(\frac{87}{8} + \frac{5}{8}\beta^2\right) \log\left|\frac{1+\beta}{1-\beta}\right| \quad (108)$$

$$\tilde{F}_{10} = \frac{41}{24}\beta + \frac{11}{12}\beta\frac{\hat{s}}{M_\Phi^2} + \left(\frac{7}{4} + \frac{1}{8}\beta^2\right) \log\left|\frac{1+\beta}{1-\beta}\right| \quad (109)$$

$$\tilde{F}_{11} = -\frac{41}{6}\beta + \frac{23}{6}\beta\frac{\hat{s}}{M_\Phi^2} + \frac{1}{2}(1-\beta^2) \log\left|\frac{1+\beta}{1-\beta}\right| \quad (110)$$

$$\tilde{F}_{12} = \frac{41}{4}\beta + \frac{43}{48}\beta\frac{\hat{s}}{M_\Phi^2} + \frac{145}{96}\beta\frac{\hat{s}^2}{M_\Phi^4} - \left(12 - \frac{3}{4}\beta^2 + \frac{1}{4}\frac{\hat{s}}{M_V^2}\right) \log\left|\frac{1+\beta}{1-\beta}\right| \quad (111)$$

$$\tilde{F}_{13} = -\frac{41}{6}\beta - \frac{355}{24}\beta\frac{\hat{s}}{M_V^2} + \frac{37}{16}\beta\frac{\hat{s}^2}{M_\Phi^4} + \left(\frac{31}{2} - \frac{1}{2}\beta^2\right) \log\left|\frac{1+\beta}{1-\beta}\right| \quad (112)$$

$$\tilde{F}_{14} = \frac{41}{24}\beta + \frac{37}{4}\beta\frac{\hat{s}}{M_\Phi^2} - \frac{113}{32}\beta\frac{\hat{s}^2}{M_\Phi^4} + \frac{49}{96}\beta\frac{\hat{s}^3}{M_\Phi^6} - \left(\frac{23}{4} - \frac{1}{8}\beta^2 + \frac{1}{4}\frac{\hat{s}}{M_\Phi^2}\right) \log\left|\frac{1+\beta}{1-\beta}\right|. \quad (113)$$

$$(114)$$

Finally, the coefficients for the differential and the integrated cross section for  $q\bar{q} \rightarrow V\bar{V}$ ,  $G_i(\hat{s}, \beta, \cos\theta)$  and  $\tilde{G}_i(\hat{s}, \beta)$ , are given by

$$G_0 = 1 + \frac{1}{16} \left[ \frac{\hat{s}}{M_\Phi^2} - (1 + 3\beta^2) \right] \sin^2\theta \quad (115)$$

$$G_1 = -1 - \frac{1}{8} \left[ \frac{\hat{s}}{M_\Phi^2} - 2 \right] \sin^2\theta \quad (116)$$

$$G_2 = 1 \quad (117)$$

$$G_3 = \frac{1}{4} + \frac{1}{16} \left[ \frac{\hat{s}}{M_\Phi^2} - 2 \right] \sin^2\theta \quad (118)$$

$$G_4 = -\frac{1}{2} + \frac{1}{4} \sin^2\theta \quad (119)$$

$$G_5 = \frac{1}{4} + \frac{1}{8} \left[ \frac{\hat{s}}{M_\Phi^2} - 1 \right] \sin^2\theta \quad (120)$$

$$\tilde{G}_0 = \frac{1}{24} \frac{\hat{s}}{M_\Phi^2} + \frac{23 - 3\beta^2}{24} \quad (121)$$

$$\tilde{G}_1 = -\frac{1}{12} \frac{\hat{s}}{M_\Phi^2} - \frac{5}{6} \quad (122)$$

$$\tilde{G}_2 = 1 \quad (123)$$

$$\tilde{G}_3 = \frac{1}{24} \frac{\hat{s}}{M_\Phi^2} + \frac{1}{6} \quad (124)$$

$$\tilde{G}_4 = -\frac{1}{3} \quad (125)$$

$$\tilde{G}_5 = \frac{1}{12} \frac{\hat{s}}{M_\Phi^2} + \frac{1}{6}. \quad (126)$$

## References

- [1] J.C. Pati and A. Salam, Phys. Rev. **D10** (1974) 275;  
L.F. Abbott and E. Farhi, Phys. Lett. **B101** (1981) 69; Nucl. Phys. **B189** (1981) 549;  
E. Farhi and L. Susskind, Phys. Rep. **74** (1981) 277;  
L. Lyons, Progr. Part. Nucl. Phys. **10** (1982) 227;  
B. Schrempp and F. Schrempp, DESY 84-055 (1984); Phys. Lett. **B153** (1985) 101;  
W. Buchmüller, Acta Phys. Austr. Suppl. **XXVII** (1985) 517;  
J. Hewett and T.G. Rizzo, Phys. Rep. **183** (1989) 193;  
H. Murayama and T. Yanagida, Mod. Phys. Lett. **A7** (1992) 147;  
P.H. Frampton, Mod. Phys. Lett. **A7** (1992) 559.
- [2] For reviews see:  
P. Langacker, Phys. Rep. **72** (1981) 185;  
G.G. Ross, *Grand Unified Theories* (Benjamin, Reading, MA, 1984).
- [3] W. Buchmüller and D. Wyler, Phys. Lett. **B177** (1986) 377;  
M. Leurer, Phys. Rev. Lett. **71** (1993) 1324; Phys. Rev. **D49** (1994) 333; Phys. Rev. **D50** (1994) 536;  
S. Davidson, D. Bailey, and B.A. Campbell, Z. Phys. **C61** (1994) 613;  
G. Couture and H. König, Phys. Rev. **D53** (1996) 555.
- [4] D. Alexander et al., OPAL collaboration, Phys. Lett. **B275** (1992) 123; Phys. Lett. **B263** (1991) 123;  
D. Decamp et al., ALEPH collaboration, Phys. Rep. **216** (1992) 253;  
B. Adeva et al., L3 collaboration, Phys. Lett. **B261** (1991) 169; O. Adriani, L3 collaboration, Phys. Rep. **236** (1993) 1;  
P. Abreu et al., DELPHI collaboration, Phys. Lett. **B275** (1992) 222; **B316** (1993) 620;  
J.K. Mizukoshi, O.J.P. Eboli, and M.C. Gonzalez-Garcia, Nucl. Phys. **B443** (1995) 20.
- [5] M. Derrick et al., ZEUS collaboration, Phys. Lett. **B306** (1993) 173; DESY 94-204-F;  
I. Abt et al., H1 collaboration, Nucl. Phys. **B396** (1993) 3;  
T. Ahmed et al., H1 collaboration, Z. Phys. **C64** (1994) 545;  
S. Aid et al., H1 collaboration, Phys. Lett. **B353** (1995) 578; **B369** (1996) 173;  
M. Derrick et al., ZEUS collaboration, DESY 96-161.
- [6] F. Abe et al., CDF collaboration, Phys. Rev. **D48** (1993) R3939; Phys. Rev. Lett. **75** (1995) 1012;  
S. Abachi et al., D0 collaboration, Phys. Rev. Lett. **72** (1994) 965; **75** (1995) 3618.
- [7] H.J. Behrend et al., CELLO collaboration, Phys. Lett. **B178** (1986) 452, A: **184** (1987) 417;  
W. Bartel et al., JADE collaboration, Z. Phys. **C36** (1987) 15;  
J. Alitti et al., UA2 collaboration, Phys. Lett. **B274** (1992) 507.
- [8] Review of Particle Physics, Phys. Rev. **D54** (1996) 235. The mass limits on first and second generation scalar leptoquarks are 97 GeV and 116 GeV at 95% CL, respectively.
- [9] J. Hewett and S. Pakvasa, Phys. Lett. **B227** (1989) 178;  
T.M. Aliev and A.A. Bayramov, Sov. J. Nucl. Phys. **52** (1990) 689;

- T.G. Rizzo, Phys. Rev. **D44** (1991) 186;  
T.M. Aliev and Kh. A. Mustafaev, Yad. Fiz. **53** (1991) 771;  
J.E. Cieza Montalvo and O.J.P. Eboli, Phys. Rev. **D47** (1993) 837;  
H. Nadeau and D. London, Phys. Rev. **D47** (1993) 3742;  
G. Belanger, D. London and H. Nadeau, Phys. Rev. **D49** (1994) 3140;  
S. Atag, A. Celikel, and S. Sultansoy, Phys. Lett. **B326** (1994) 185;  
O. Cakir and S. Atag, J. Phys. **G21** (1995) 1189;  
V. Ilin, A. Pukhov, V. Savrin, A. Semenov, and W. von Schlippe, INP-MSU-95-22-386;  
hep-ph/9506334; Phys. Lett. **B351** (1995) 504;  
T.M. Aliev, D.A. Demir, E. Iltan, and N.K. Pak, METU-PHYS-HEP-95-14,  
hep-ph/9511389;  
F. Cuypers, MPI-PHT-95-129 (1996), hep-ph/9602355; Nucl. Phys. **B474** (1996) 57;  
T.M. Aliev, E. Iltan, and N.K. Pak, Phys. Rev. **D54** (1996) 4263;  
M.A. Doncheski and S. Godfrey, OCIP-C-96-1; hep-ph/9608368; Phys. Rev. **D49** (1994)  
6220; Phys. Rev. **D51** (1995) 1040.
- [10] J. Ohnemus, S. Rudaz, T.F. Walsh, and P.M. Zerwas, Phys. Lett. **334** (1994) 203.
- [11] J. Blümlein, E. Boos, and A. Pukhov, Mod. Phys. Lett. **A9** (1994) 3007.
- [12] J. Blümlein, DESY 93–132, Proc. of the 2nd Workshop 'Physics and Experiments with Linear  $e^+e^-$  Colliders', Waikoloa, HI, April 26–30, 1993, eds. F.A. Harris, S. Olsen, S. Pakvasa, and X. Tata, (World Scientific, Singapore, 1993) Vol. **II**, p. 524;  
DESY 93–153, Proc. of the Workshop, ' $e^+e^-$  Collisions at 500 GeV', Munich–Annecy–Hamburg, 1993, ed. P. Zerwas, (DESY, Hamburg, 1993), p. 419.
- [13] J. Blümlein and E. Boos, Nucl. Phys. **B** (Proc. Suppl.), eds. T. Riemann and J. Blümlein, **37B** (1994) p. 181, and references therein.
- [14] J. Blümlein, E. Boos, and A. Kryukov, Program description LQPAIR 1.0, in preparation.
- [15] J. Blümlein and R. Rückl, Phys. Lett. **B304** (1993) 337.
- [16] W. Buchmüller, R. Rückl, and D. Wyler, Phys. Lett. **B191** (1987) 442.
- [17] Dong-pei Zhu, Phys. Rev. **B22** (1980) 2266.
- [18] J.A. Grifols and A. Méndez, Phys. Rev. **D26** (1982) 324;  
I. Antoniadis, L. Baulieu, and F. Delduc, Z. Phys. **C23** (1984) 119;  
E. Eichten, I. Hinchliffe, K. Lane, and C. Quigg, Rev. Mod. Phys. **56** (1984) 579;  
G. Altarelli and R. Rückl, Phys. Lett. **B144** (1984) 126;  
S. Dawson, E. Eichten, and C. Quigg, Phys. Rev. **D31** (1985) 1581.
- [19] P. Arnold and C. Wendt, Phys. Rev. **D33** (1986) 1873.
- [20] P.R. Harrison and C.H. Llewellyn Smith, Nucl. Phys. **B213** (1983) 223; E: **B223** (1983) 524.
- [21] G.V. Borisov, Y.F. Pirogov, and K.R. Rudakov, Z. Phys. **C36** (1987) 217.
- [22] M. de Montigny and L. Marleau, Can. J. Phys. **68** (1990) 612.

- [23] M. de Montigny, L. Marleau, and G. Simon, Phys. Rev. **D52** (1995) 533.
- [24] J.L. Hewett and S. Pakvasa, Phys. Rev. **D37** (1988) 3165.
- [25] J.E. Cieza–Montalvo and O.J.P. Eboli, Phys. Rev. **D50** (1994) 331.
- [26] N. Cabibbo and R. Gatto, Phys. Rev. **124** (1961) 1577.
- [27] E. Boos et al., Proc of the XXVIth Rencontre de Moriond, ed. I. Tran Than Van, (Edition Frontiers, Paris, 1991), p. 501;  
 E. Boos et al., Proc of the 2nd Int. Workshop on Software Engineering, ed. D. Perret–Gallix, (World Scientific, Singapore, 1992), p. 665;  
 E. Boos et al., KEK–preprint 92–47, 1992;  
 E. Boos, M. Dubinin, V. Ilyin, A. Pukhov, and V. Savrin, hep-ph/9503280, SNUTP-94-116;  
 E. Boos et al., in: Proc. of the Xth Int. Workshop on High Energy Physics and Quantum Field Theory, QFTHEP–95, ed. by B. Levtchenko, and V. Savrin, (Moscow, 1995), p. 101.
- [28] J.A.M. Vermaseren, Symbolic Manipulation with FORM, version 2, (CAN, Amsterdam, 1991).
- [29] W. Alles, Ch. Boyer, and A.J. Buras, Nucl. Phys. **B119** (1977) 125.
- [30] S. Frixione, M. Mangano, P. Nason, and G. Ridolfi, Phys. Lett. **B319** (1993) 339.
- [31] I.F. Ginzburg, G.L. Kotkin, V.G. Serbo, and V.I. Telnov, Nucl. Inst. Meth. **205** (1983) 47.
- [32] I.F. Ginzburg, private communication.
- [33] H.L. Lai, J. Botts, J. Huston, J.G. Morfin, J.F. Owens, J.W. Qiu, W.K. Tung, and H. Weerts, Phys. Rev. **D51** (1995) 4763.
- [34] M. Glück, E. Reya, and A. Vogt, Z. Physik **C67** (1995) 433;  
 A.D. Martin, W.J. Stirling, and R.G. Roberts, Phys. Lett. **B354** (1995) 155.
- [35] A. Djouadi, J. Ng, and T.G. Rizzo, SLAC–PUB–95–6772.
- [36] J.L. Hewett, T.G. Rizzo, S. Pakvasa, H.E. Haber, and A. Pomarol, in: Proc. of the Workshop ‘Physics at Current Accelerators and Supercolliders’, Argonne, June 1993, eds. J.L. Hewett, A.R. White, and D. Zeppenfeld, (ANL, Argonne, 1993), p. 539.
- [37] T.G. Rizzo, SLAC–PUB–96–7284, September 1996.
- [38] M. Glück, E. Reya, and A. Vogt, Phys. Rev. **D46** (1992) 1973.
- [39] J. Blümlein, E. Boss, and A. Kryukov, DESY 96–219, October 1996.
- [40] T. Muta, *Foundations of Quantum Chromodynamics*, (World Scientific, Singapore, 1987).



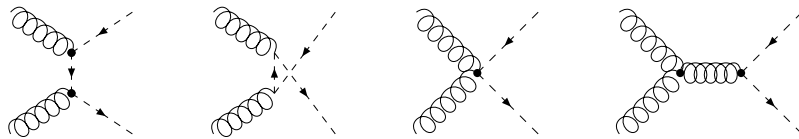


Figure 1: Diagrams describing leptoquark pair production via gluon–gluon fusion. Here the dashed lines denote both scalar and vector leptoquarks.

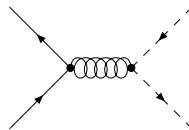


Figure 2: Diagram for the subprocess  $q\bar{q} \rightarrow \Phi_{S,V}\bar{\Phi}_{S,V}$ .

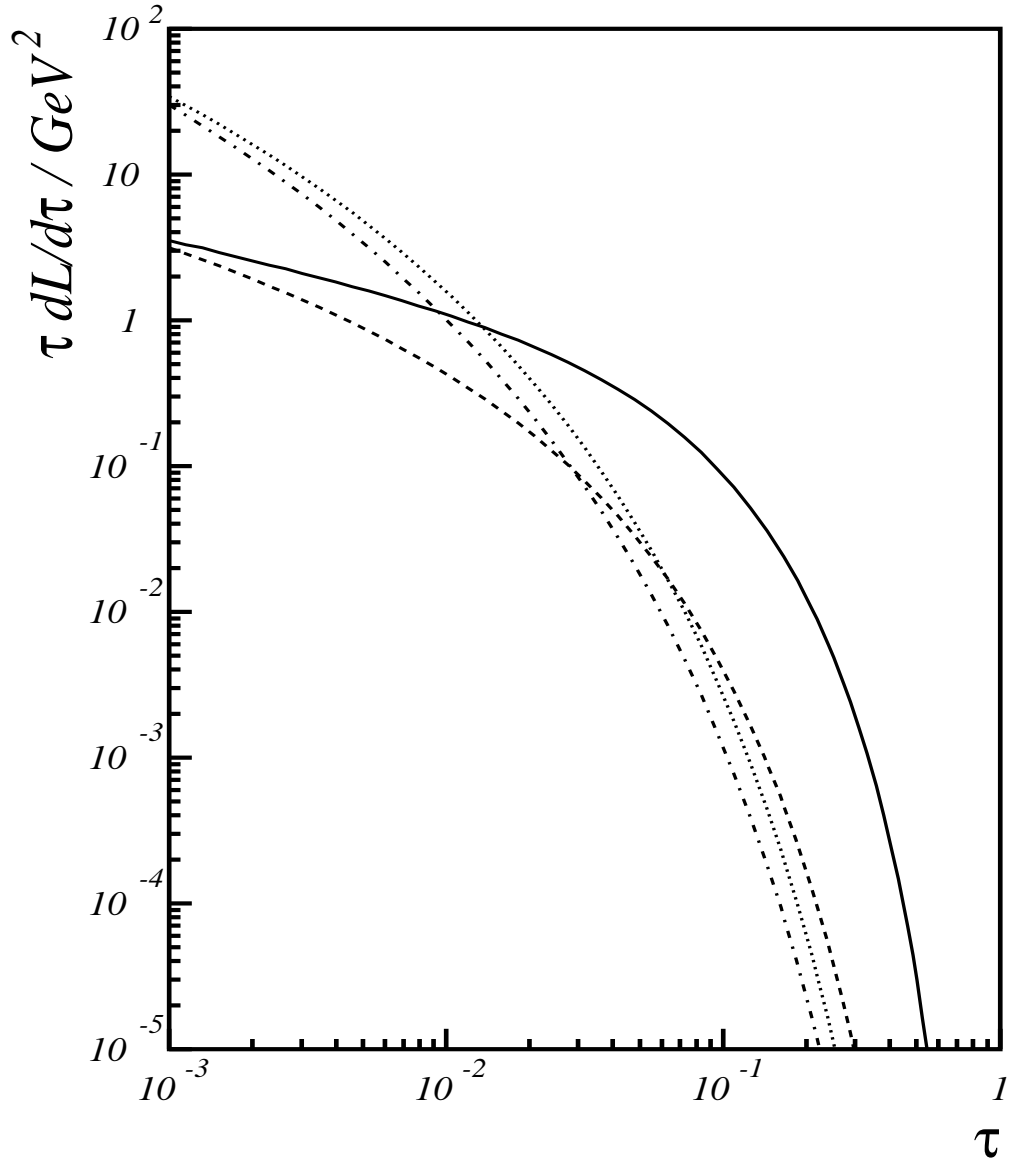


Figure 3 : Parton luminosities  $\tau d\mathcal{L}^{q,g}/d\tau$  for different hadron colliders using the CTEQ3 parametrization [33]. Full line: quark-antiquark luminosity for  $p\bar{p}$  at  $\sqrt{S} = 1.8$  TeV; dashed line: quark-antiquark luminosity for  $pp$  at  $\sqrt{S} = 14$  TeV; dotted line: gluon-gluon luminosity for  $p\bar{p}$  at  $\sqrt{S} = 1.8$  TeV; dash-dotted line: gluon-gluon luminosity for  $pp$  at  $\sqrt{S} = 14$  TeV.

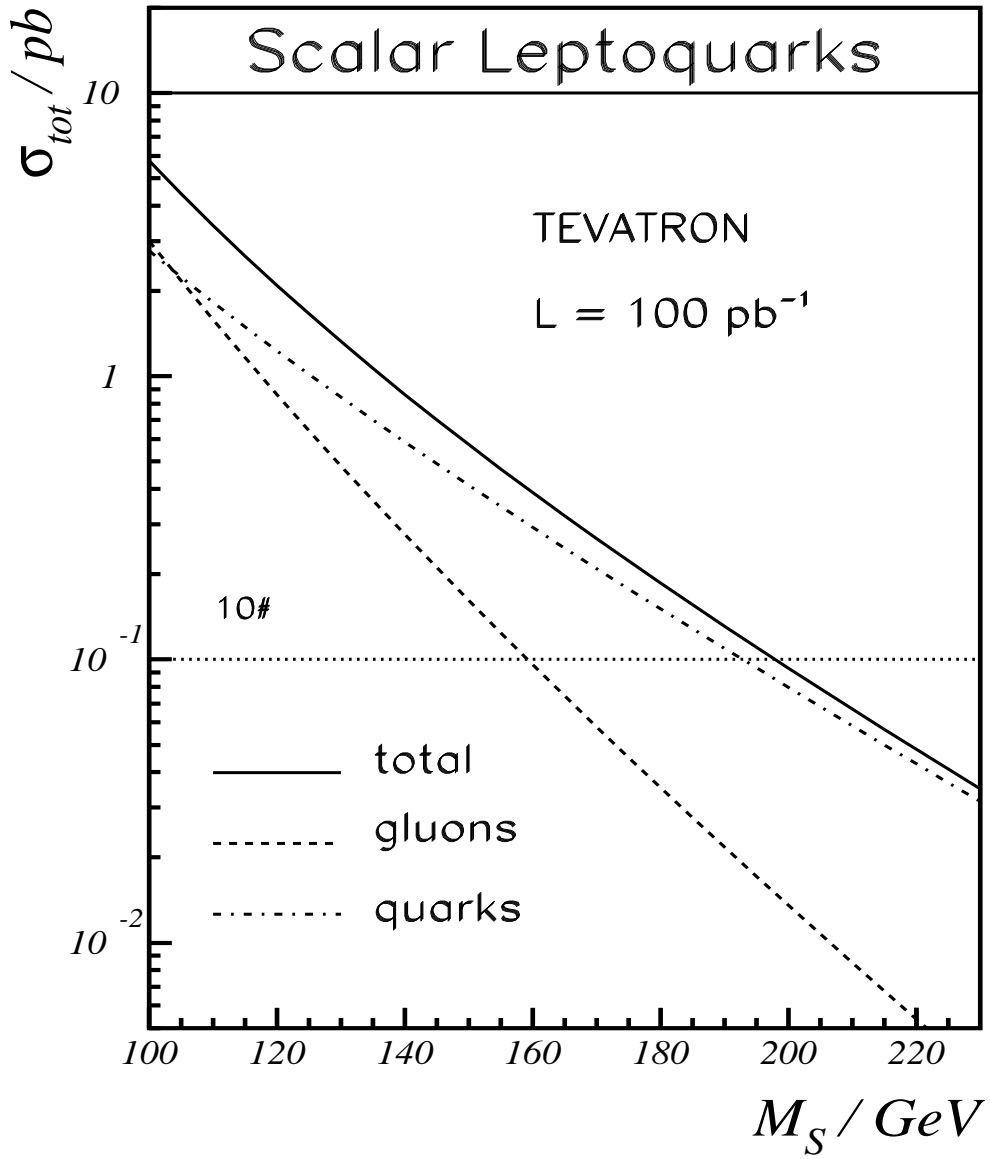


Figure 4a: Integrated cross sections for scalar leptoquark pair production at the TEVATRON,  $\sqrt{S} = 1.8$  TeV.

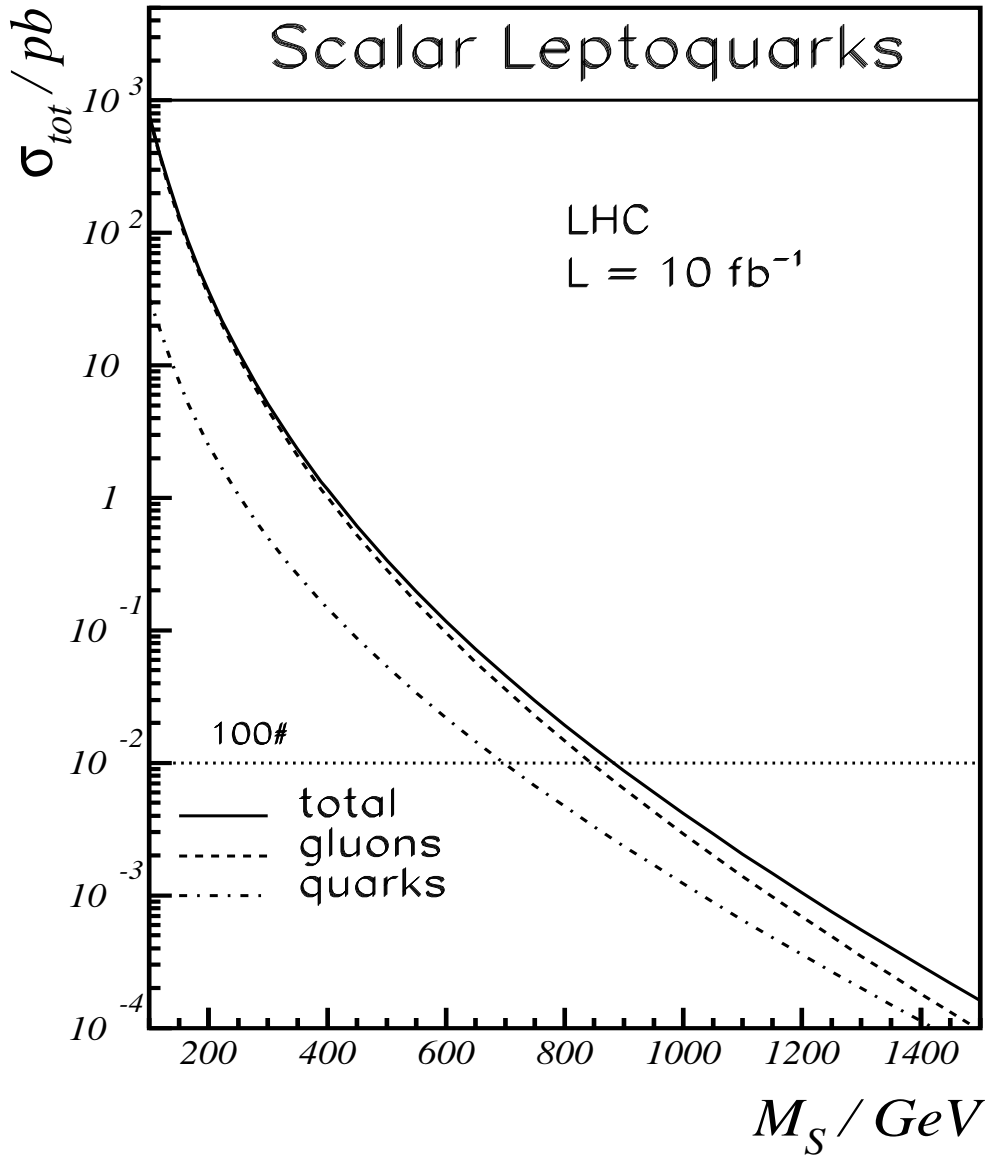


Figure 4b: Integrated cross sections for scalar leptoquark pair production at LHC,  $\sqrt{S} = 14$  TeV.

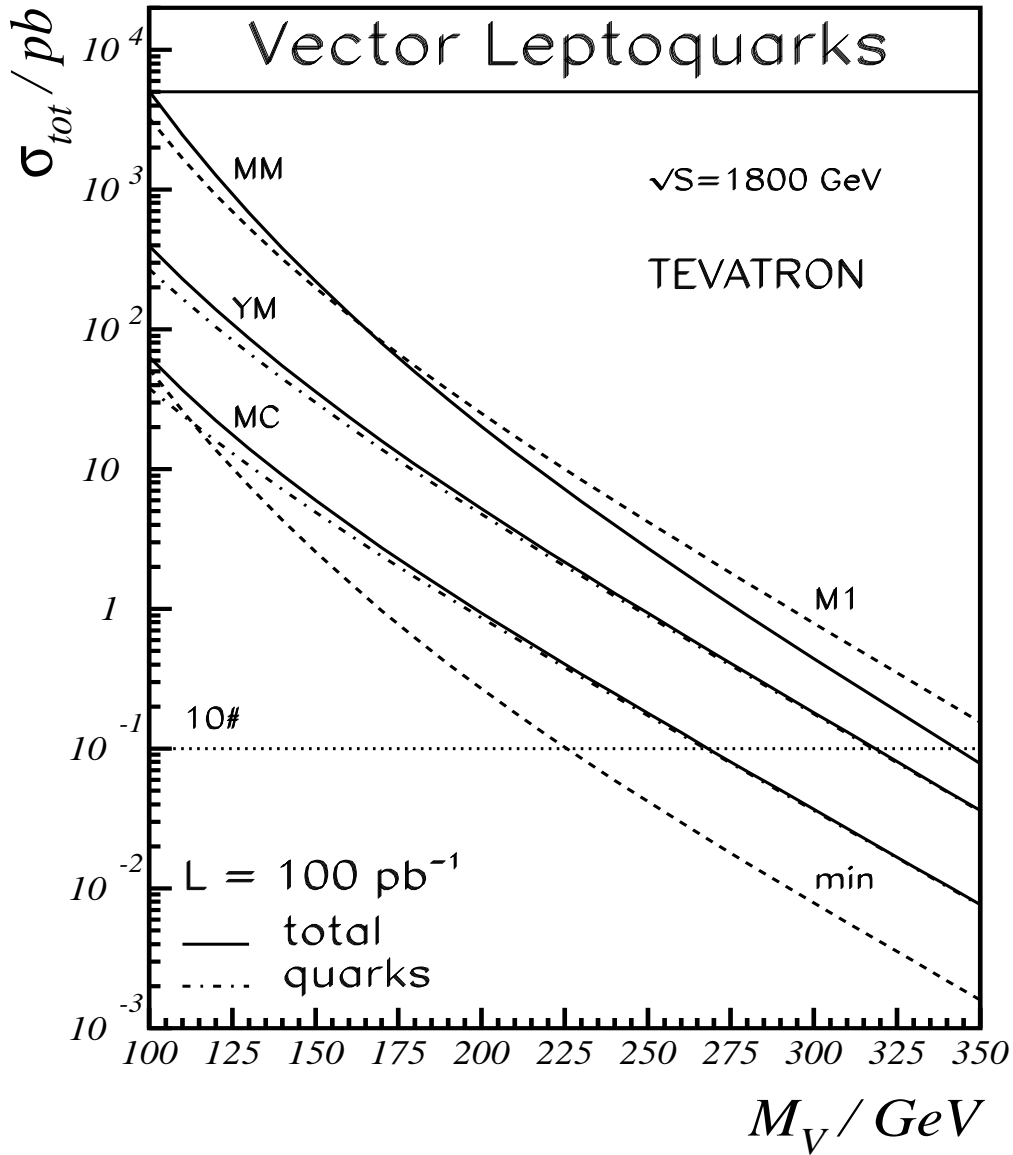


Figure 5a: Integrated cross sections for vector leptoquark pair production at the TEVATRON,  $\sqrt{S} = 1.8$  TeV. The quark contributions for the cases of a Yang-Mills type coupling (YM),  $\kappa_G = \lambda_G \equiv 0$ , and the minimal coupling  $\kappa_G = 1, \lambda_G = 0$  (MC) are shown explicitly. The upper full line denotes the total cross section for the case  $\kappa_G = \lambda_G = -1$  (MM), while the upper dashed line corresponds to  $\kappa_G = -1, \lambda_G = +1$  (M1), and the lower dashed line to  $\kappa_G = 1.3, \lambda_G = -0.21$  (min).

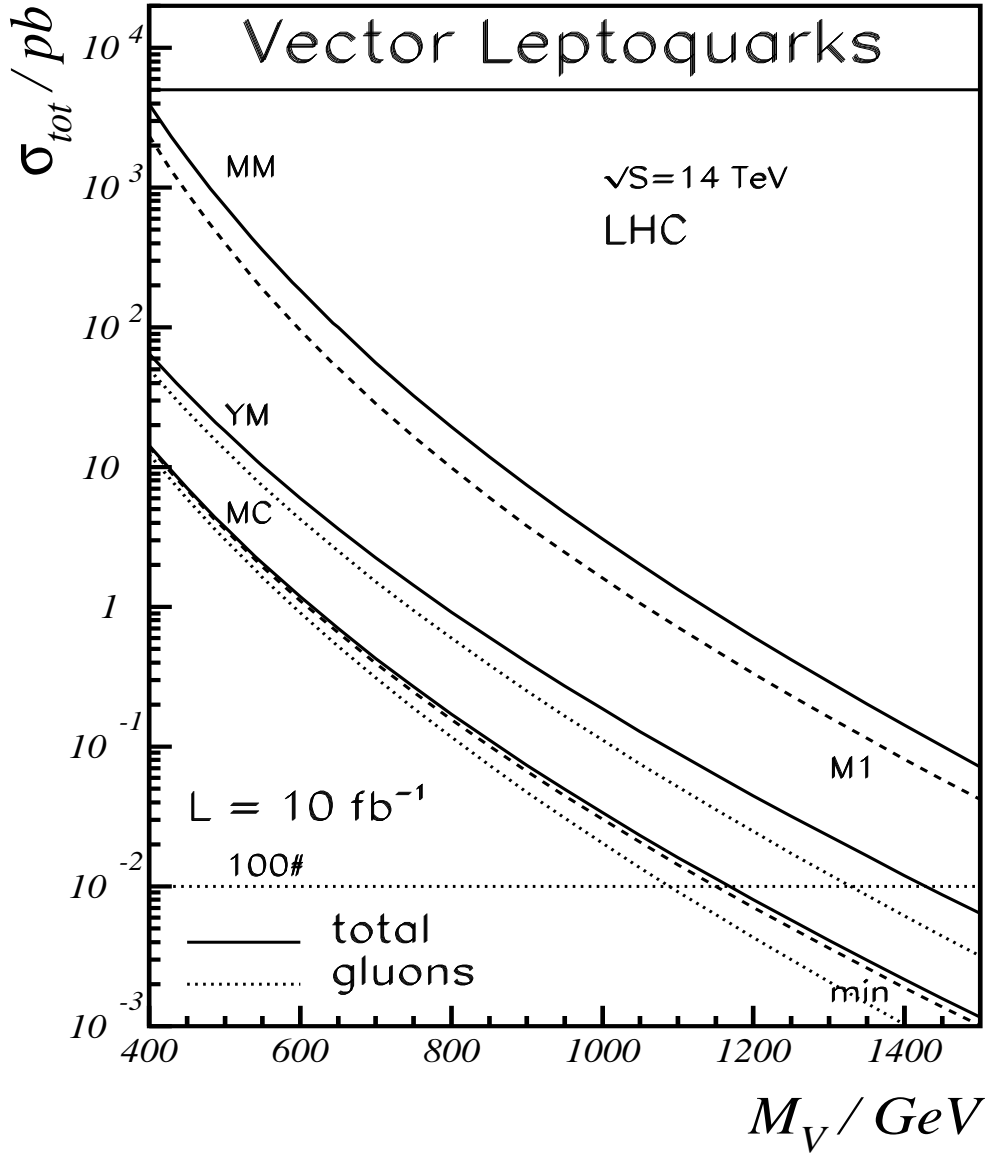


Figure 5b: Integrated cross sections for vector leptoquark pair production at LHC,  $\sqrt{S} = 14 \text{ TeV}$ . For the Yang-Mills type (YM) and minimal vector couplings (MC) also the gluon contributions are shown explicitly (dotted lines). The lower dashed line corresponds to  $\kappa_G = 1, \lambda_G = -0.05$  (min). The other notations are the same as in figure 5a.

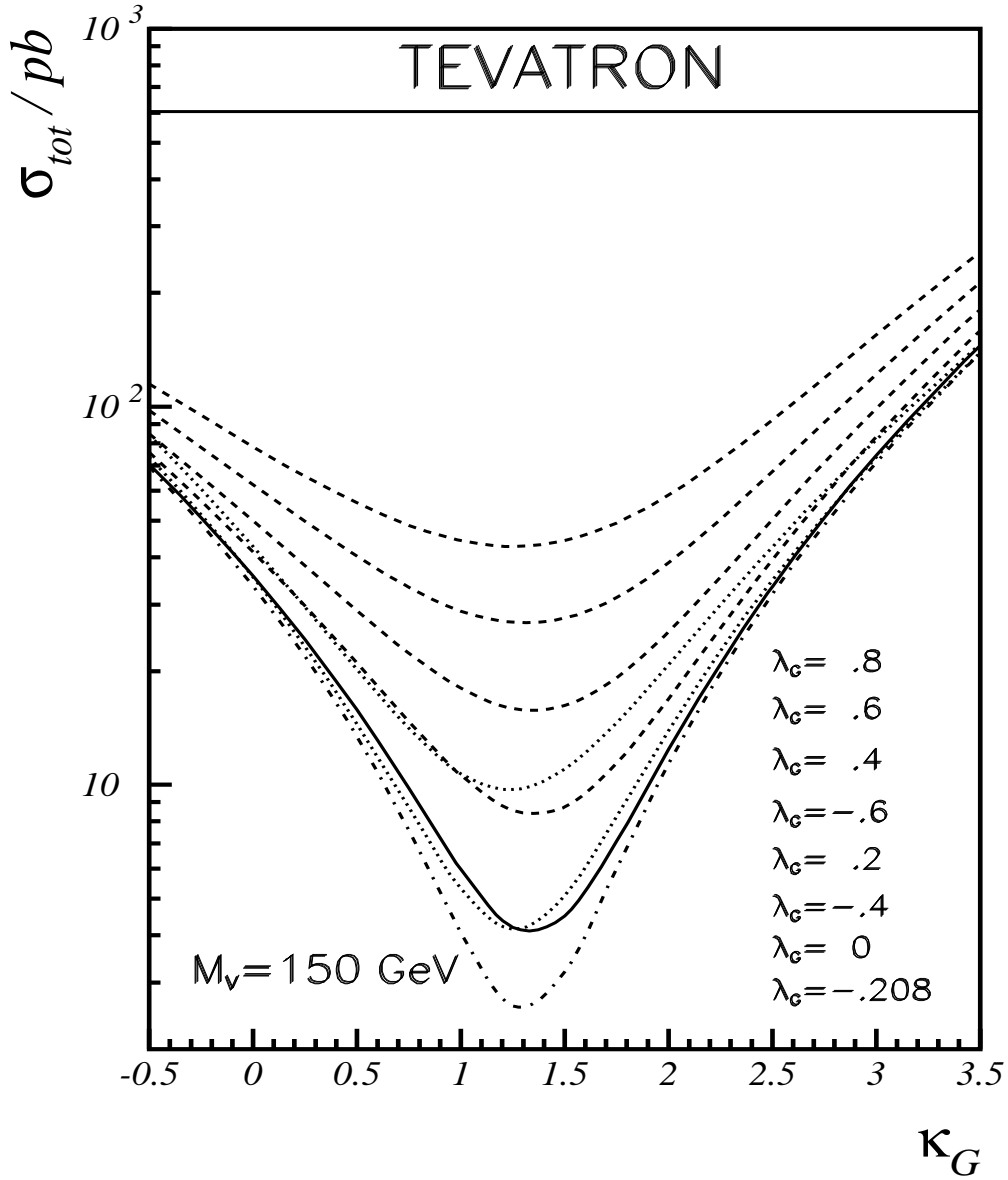


Figure 6a: Dependence of the integrated cross sections for vector leptoquark pair production on the anomalous couplings  $\kappa_G$  and  $\lambda_G$  at the TEVATRON,  $\sqrt{S} = 1.8$  TeV for  $M_V = 150$  GeV. The order of the values of  $\lambda_G$  follows the position of the respective minimum. Dashed lines:  $\lambda_G > 0$ , dotted lines:  $\lambda_G < 0$ , full line:  $\lambda_G = 0$ , dash-dotted line:  $\lambda_G = -0.208$ .

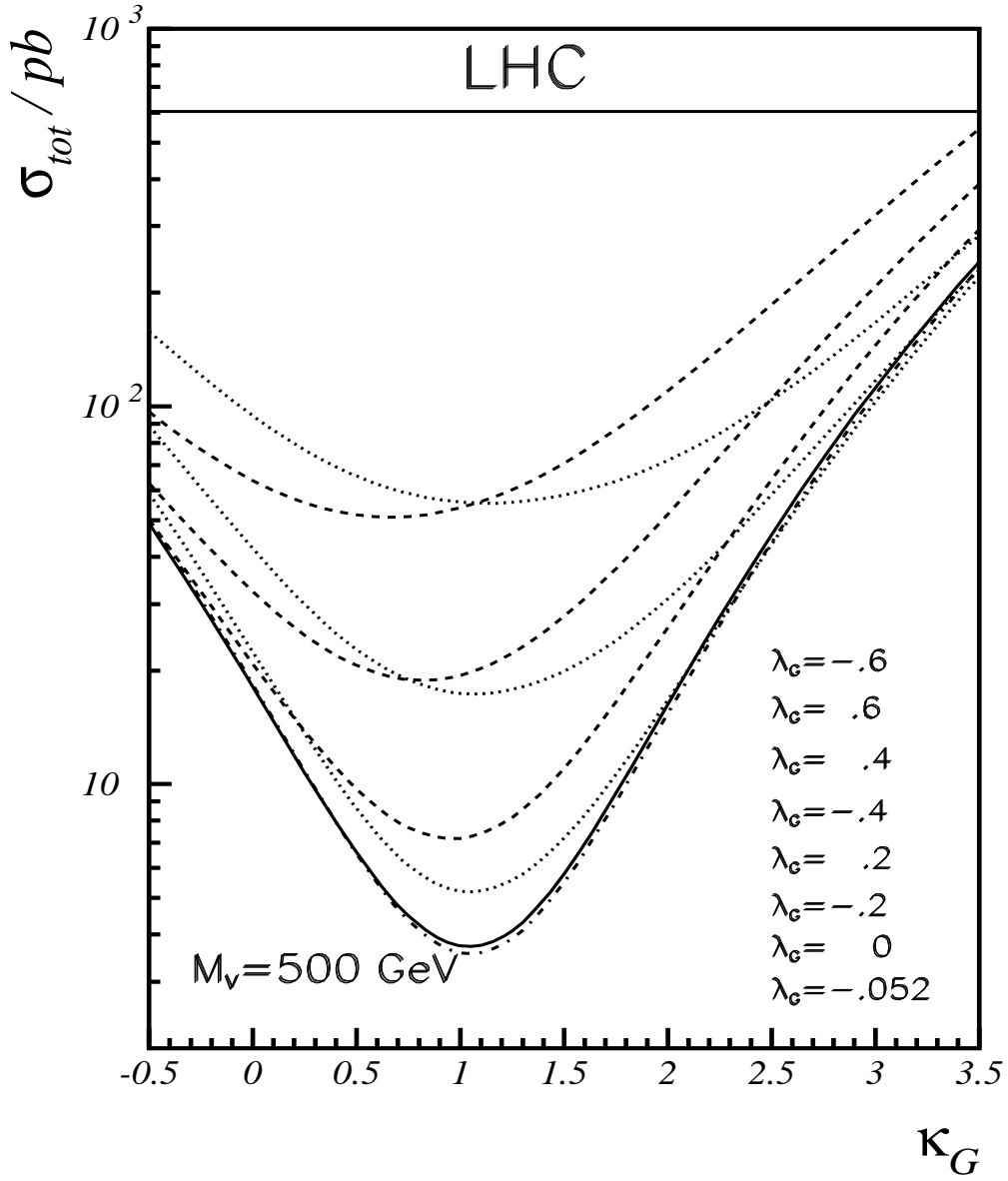


Figure 6b: Dependence of the integrated cross sections for vector leptoquark pair production on the anomalous couplings  $\kappa_G$  and  $\lambda_G$  at LHC,  $\sqrt{S} = 14$  TeV for  $M_V = 500$  GeV. The dash-dotted line corresponds to  $\lambda_G = -0.052$ . The other parameters are the same as in figure 6a.



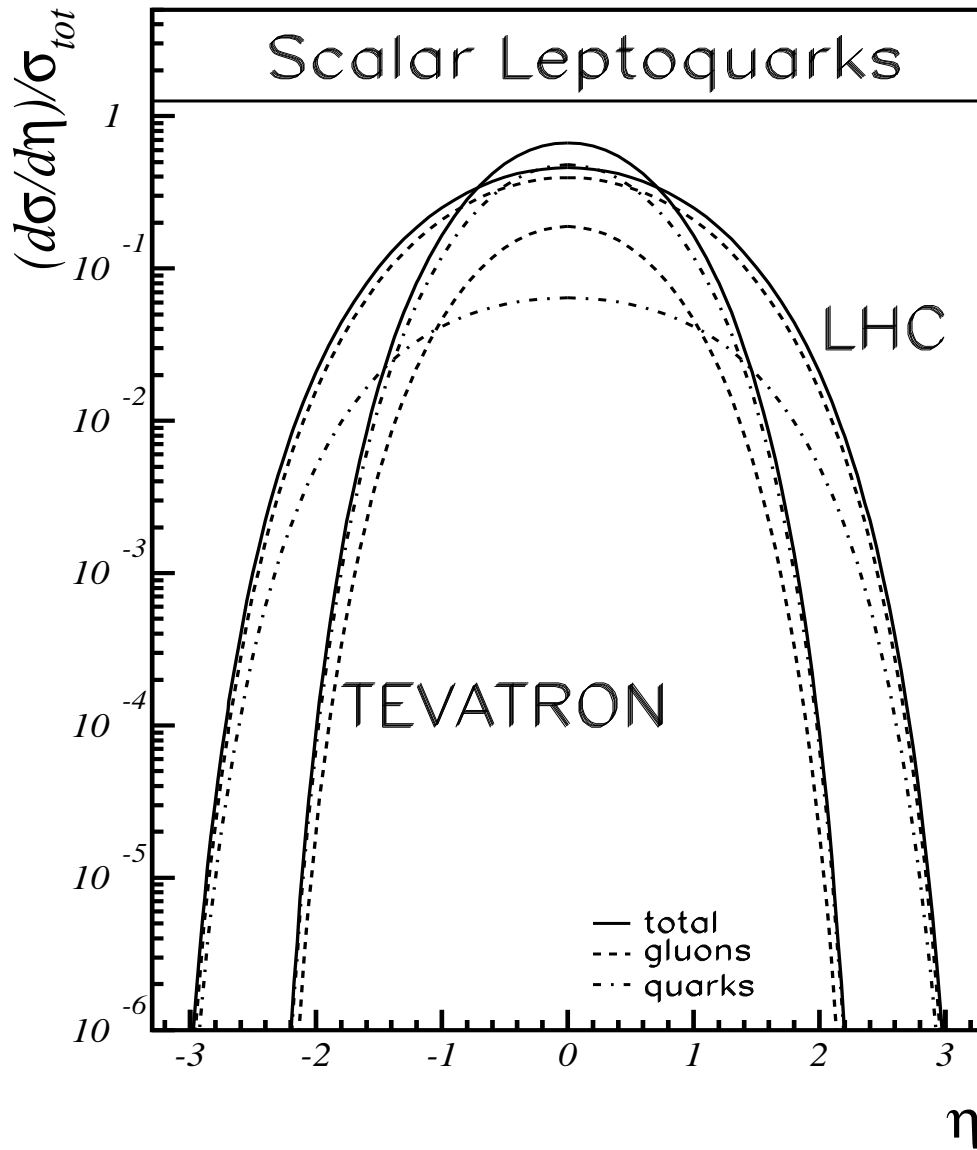


Figure 7a: Rapidity distributions for scalar leptoquark pair production at the TEVATRON and LHC. The leptoquark masses are the same as in figures 6a,b.

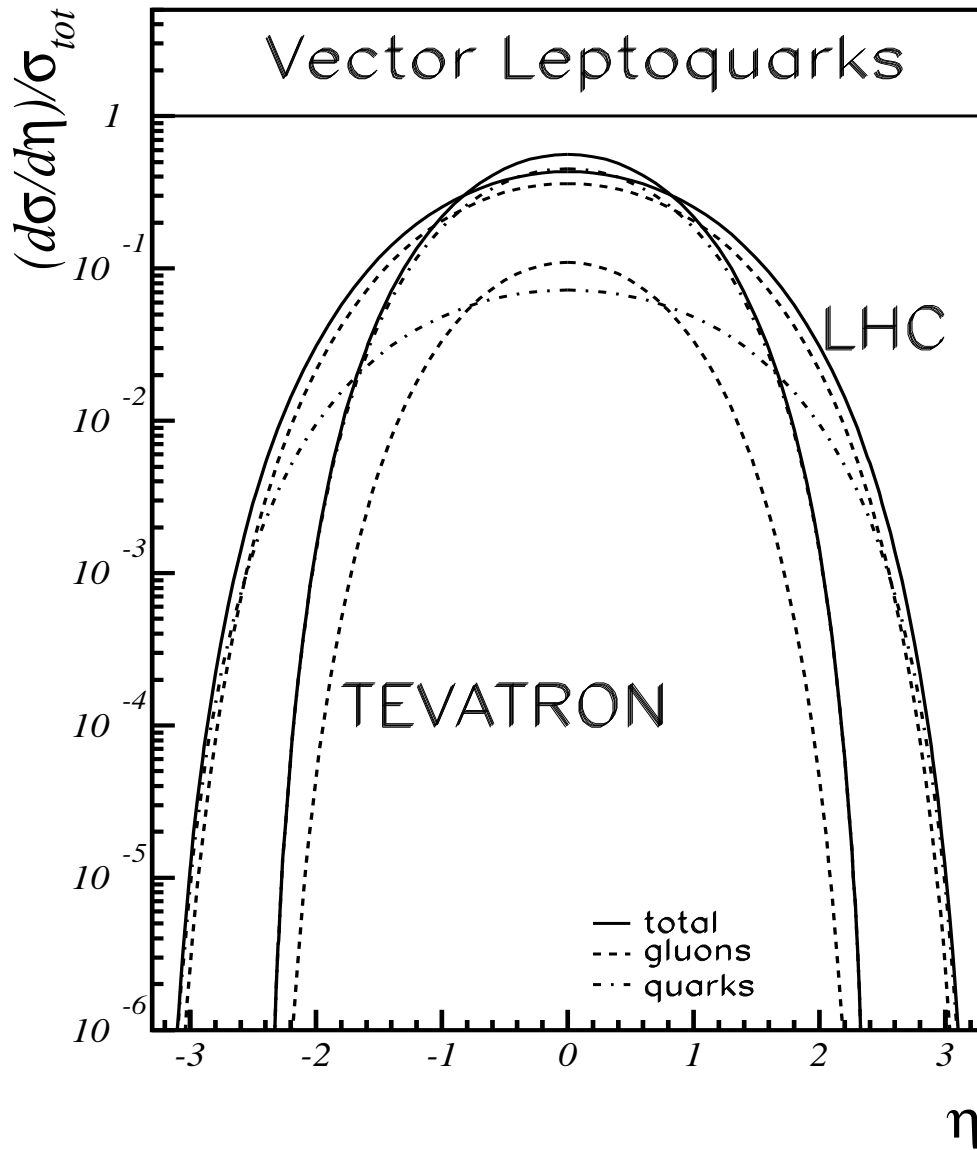


Figure 7b: Rapidity distributions for vector leptoquark pair production at the TEVATRON and LHC assuming minimal vector couplings. The notation is the same as in figure 7a.

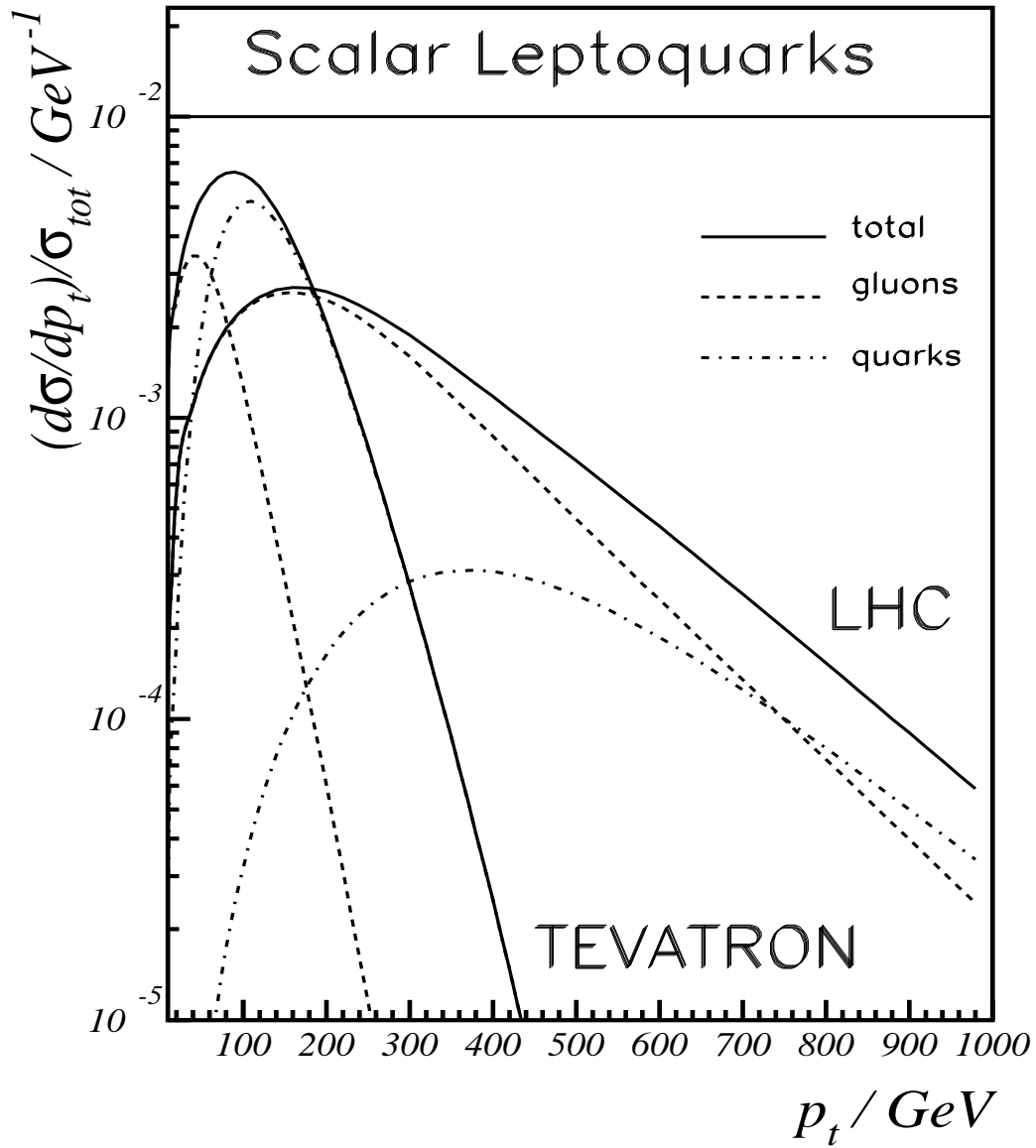


Figure 8a:  $p_{\perp}$  distributions for scalar leptoquark pair production at the TEVATRON and LHC. The leptoquark masses are the same as in figures 6a,b.

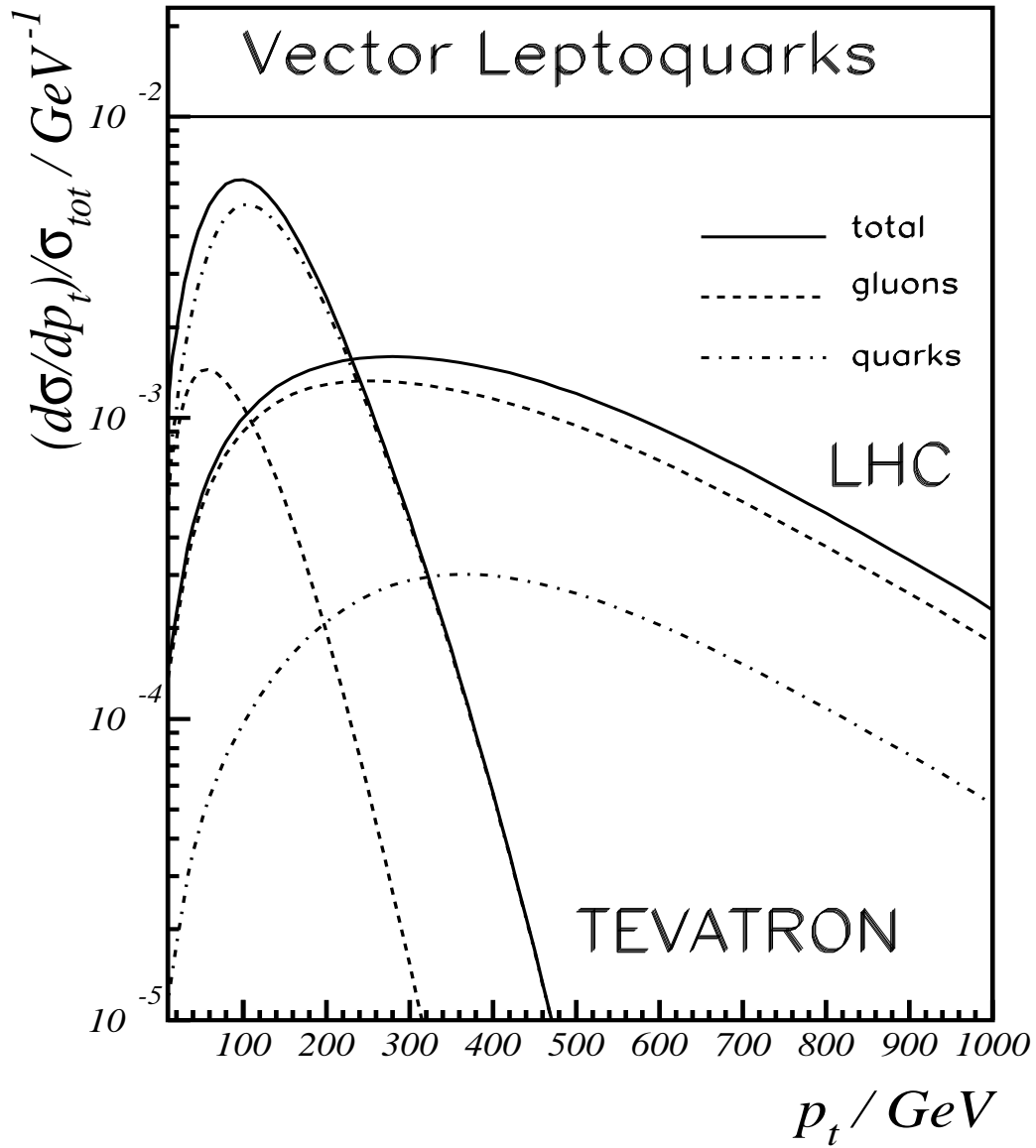


Figure 8b:  $p_{\perp}$  distributions for vector leptoquark pair production at the TEVATRON and LHC assuming minimal vector couplings. The notation is the same as in figure 8a.

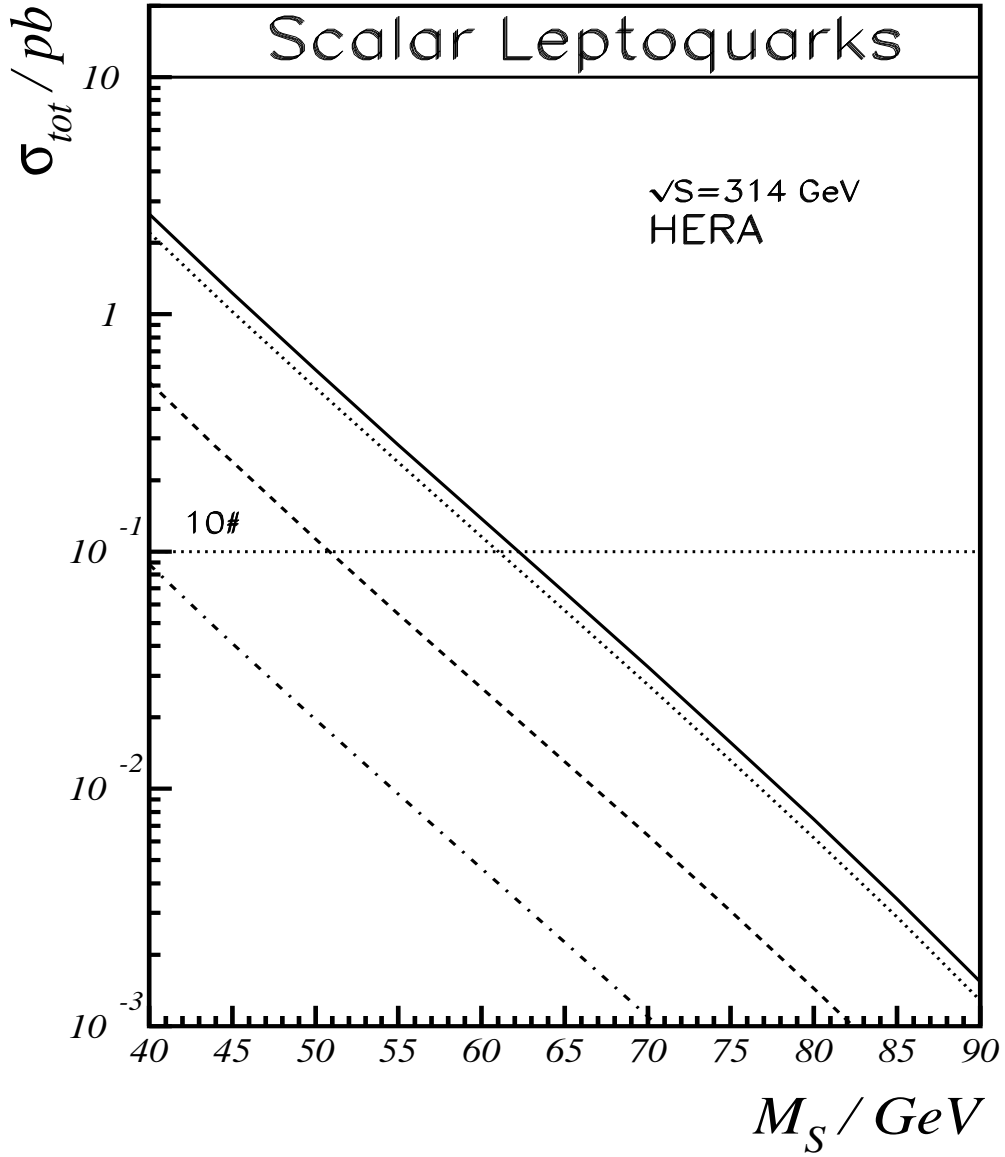


Figure 9a: Integrated cross sections for scalar leptoquark pair production at HERA,  $\sqrt{S} = 314$  GeV. Full line:  $\sigma_{tot}$  for  $|Q_\Phi| = 5/3$ ; dotted line:  $\sigma_{dir}$  for  $|Q_\Phi| = 5/3$ ; dashed line:  $\sigma_{tot}$  for  $|Q_\Phi| = 1/3$ ; dash-dotted line:  $\sigma_{dir}$  for  $|Q_\Phi| = 1/3$ .

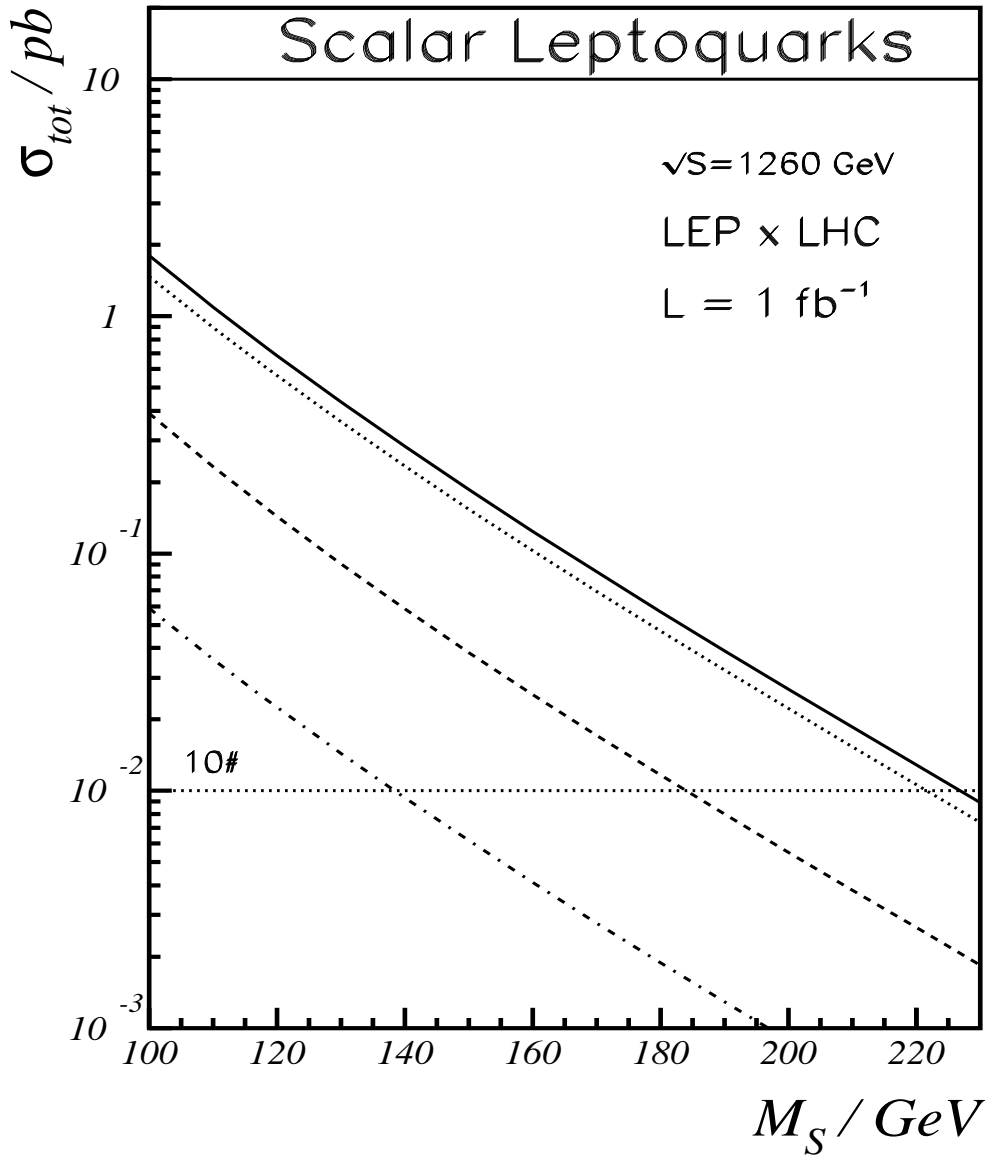


Figure 9b: Integrated cross sections for scalar leptoquark pair production at LEP  $\otimes$  LHC,  $\sqrt{S} = 1260 \text{ GeV}$ . The notations are the same as in figure 8a.

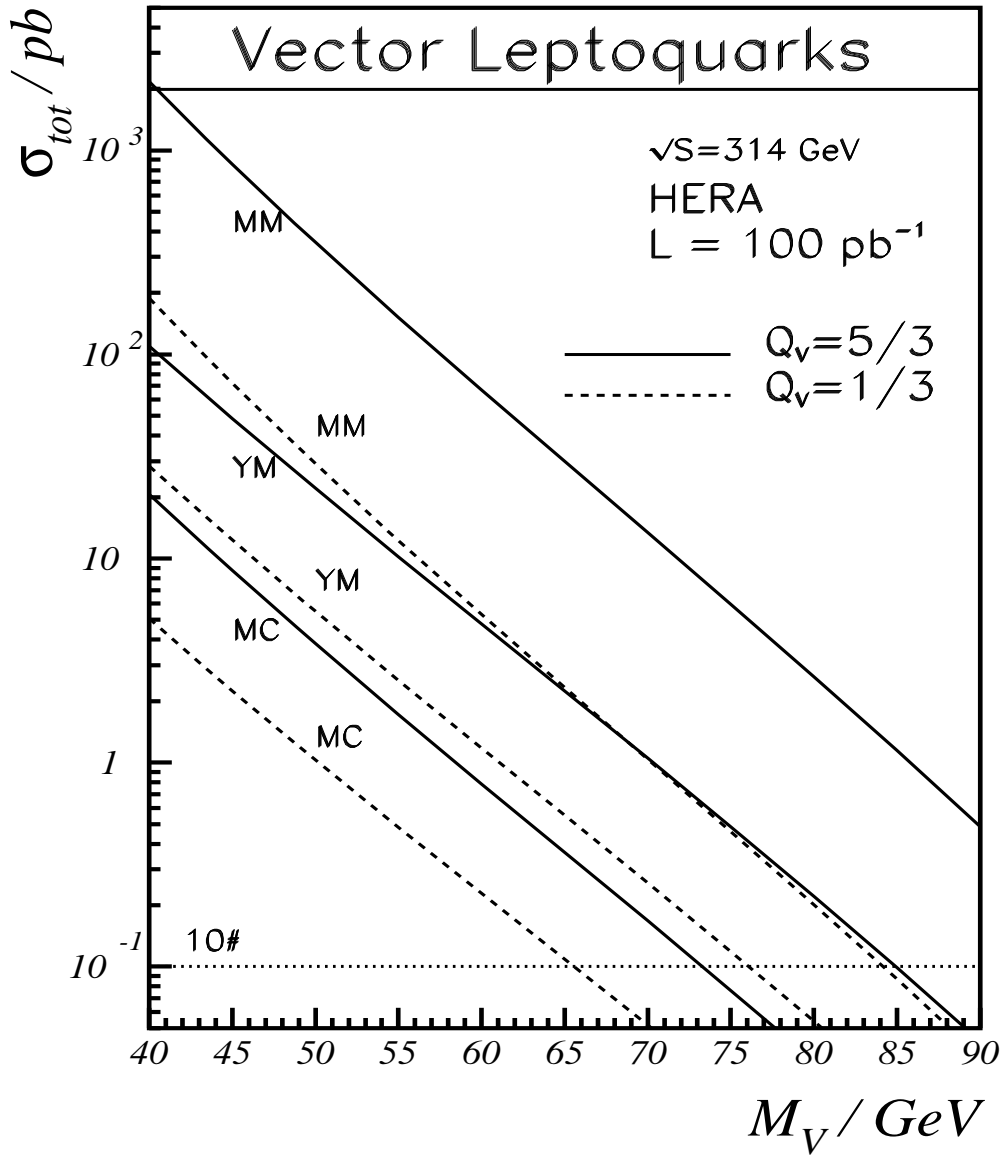


Figure 10a: Integrated cross sections  $\sigma_{tot} = \sigma_{dir} + \sigma_{res}$  for vector leptoquark pair production at HERA,  $\sqrt{S} = 314 \text{ GeV}$ . The different choices for the anomalous couplings are:  $\kappa_{G,\gamma} = \lambda_{G,\gamma} = -1$  (MM);  $\kappa_{G,\gamma} = \lambda_{G,\gamma} = 0$  (YM);  $\kappa_{G,\gamma} = 1, \lambda_{G,\gamma} = 0$  (MC).

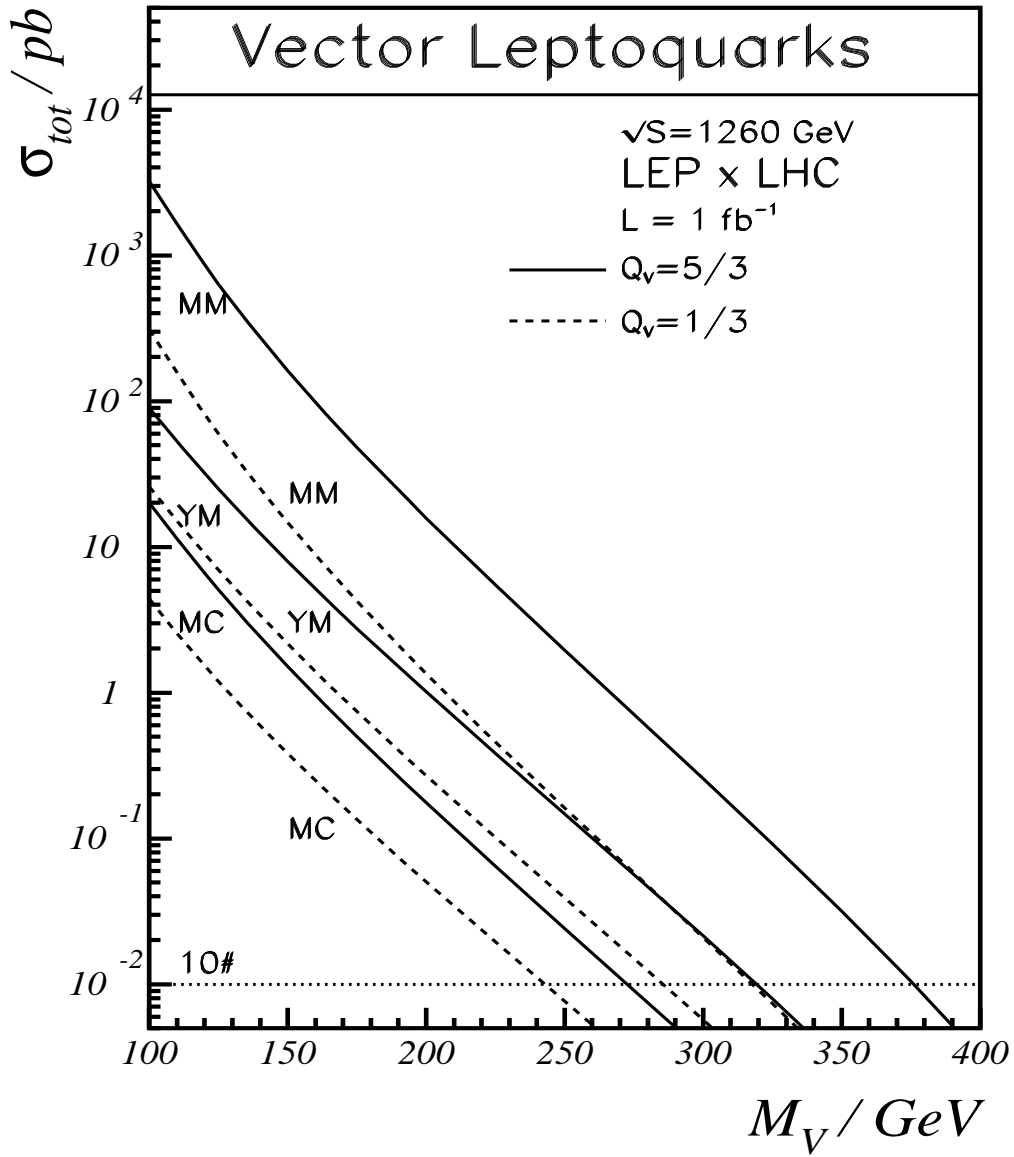


Figure 10b: Integrated cross sections for vector leptoquark pair production at LEP  $\otimes$  LHC,  $\sqrt{S} = 1260 \text{ GeV}$ . The notations are the same as in figure 9a.



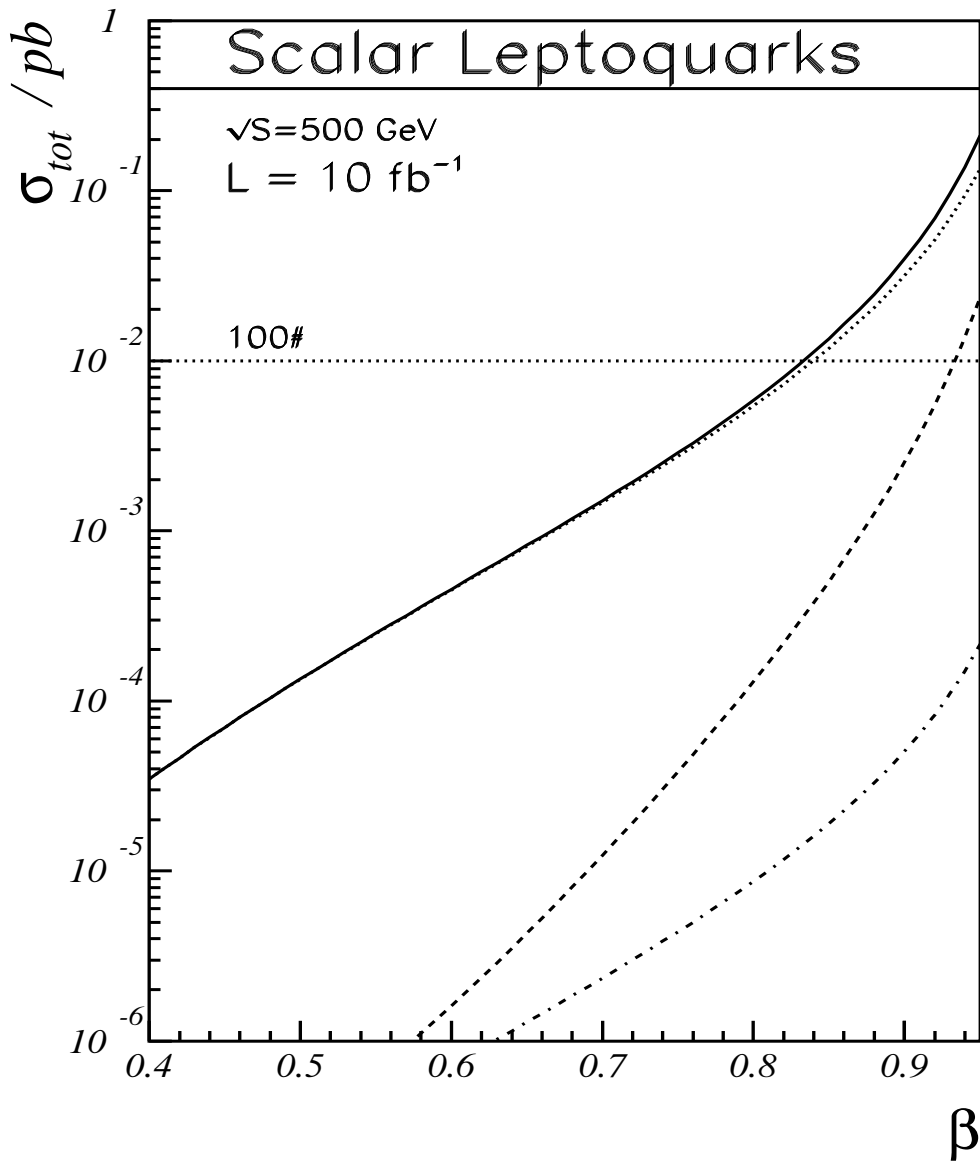


Figure 11a: Integrated cross sections for scalar leptoquark pair production through  $\gamma^*\gamma^* \rightarrow S\bar{S}$  (WWA spectrum) at future  $e^+e^-$  colliders for  $\sqrt{S} = 500 \text{ GeV}$  as a function of  $\beta$ . Full line:  $\sigma_{tot}$  for  $|Q_\Phi| = 5/3$ ; dotted line:  $\sigma_{dir}$  for  $|Q_\Phi| = 5/3$ ; dashed line:  $\sigma_{tot}$  for  $|Q_\Phi| = 1/3$ ; dash-dotted line:  $\sigma_{dir}$  for  $|Q_\Phi| = 1/3$ .

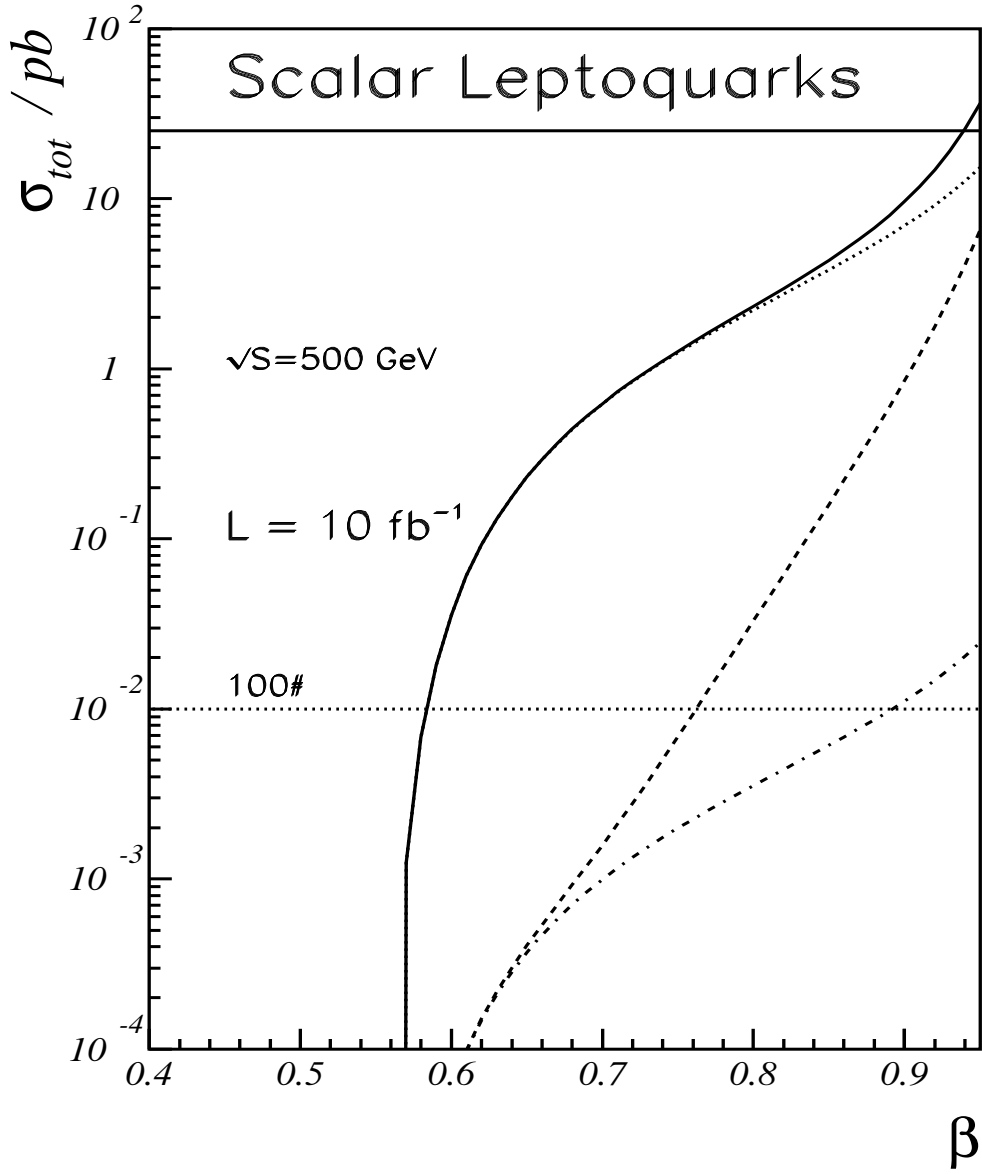


Figure 11b: Integrated cross sections for scalar leptoquark pair production at future  $\gamma\gamma$  colliders using laser back scattering for electron beam conversion. The parameters are the same as in figure 11a.

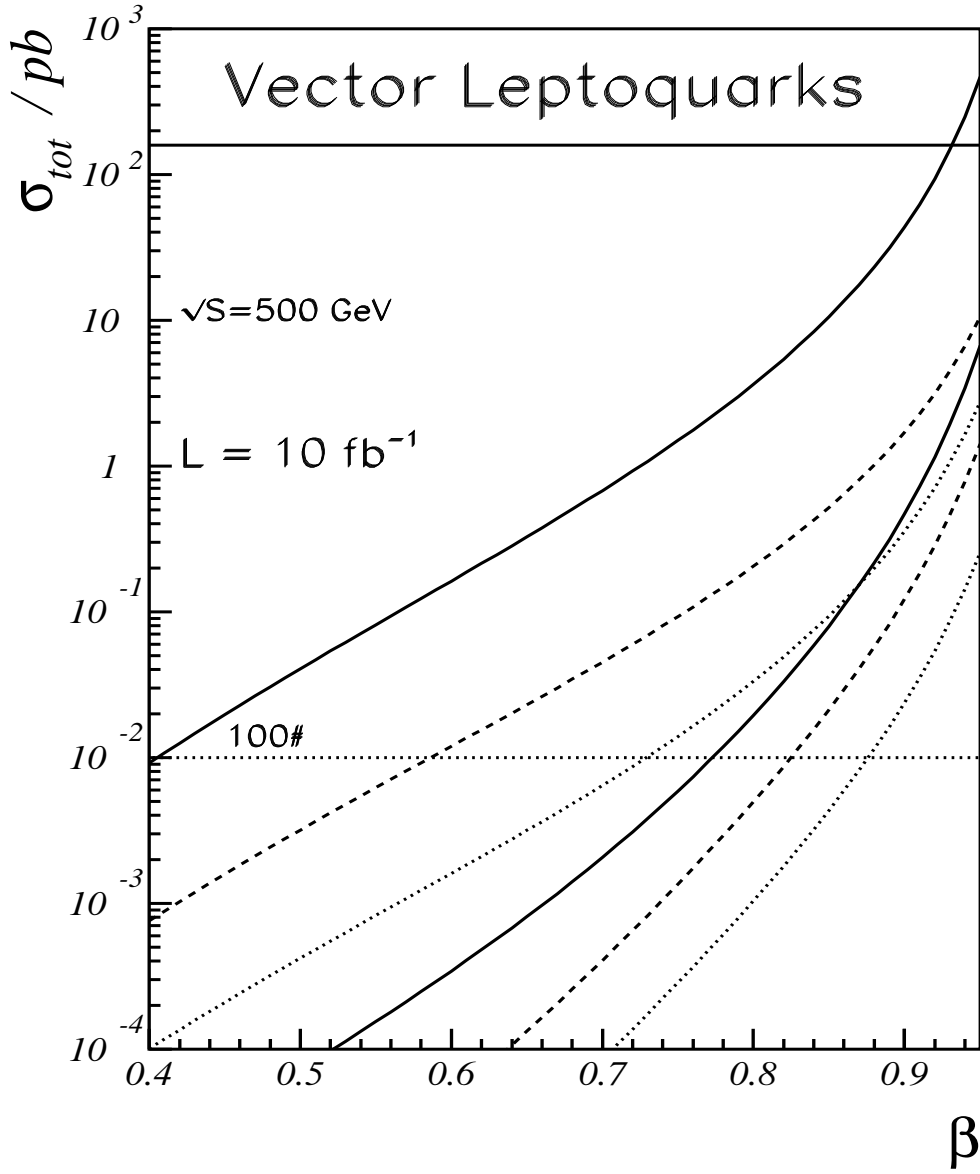


Figure 12a: Integrated cross sections for vector leptoquark pair production through  $\gamma^*\gamma^* \rightarrow V\bar{V}$  (WWA spectrum) at future  $e^+e^-$  colliders for  $\sqrt{S} = 500$  GeV as a function of  $\beta$ . Upper full line:  $|Q_\Phi| = 5/3, \kappa_{\gamma,G} = \lambda_{\gamma,G} = -1$ ; Upper dashed line:  $|Q_\Phi| = 5/3, \kappa_{\gamma,G} = \lambda_{\gamma,G} = 0$ ; Upper dotted line:  $|Q_\Phi| = 5/3, \kappa_{A,G} = 1, \lambda_{\gamma,G} = 0$ ; The corresponding lower lines represent for  $|Q_\Phi| = 1/3$ .

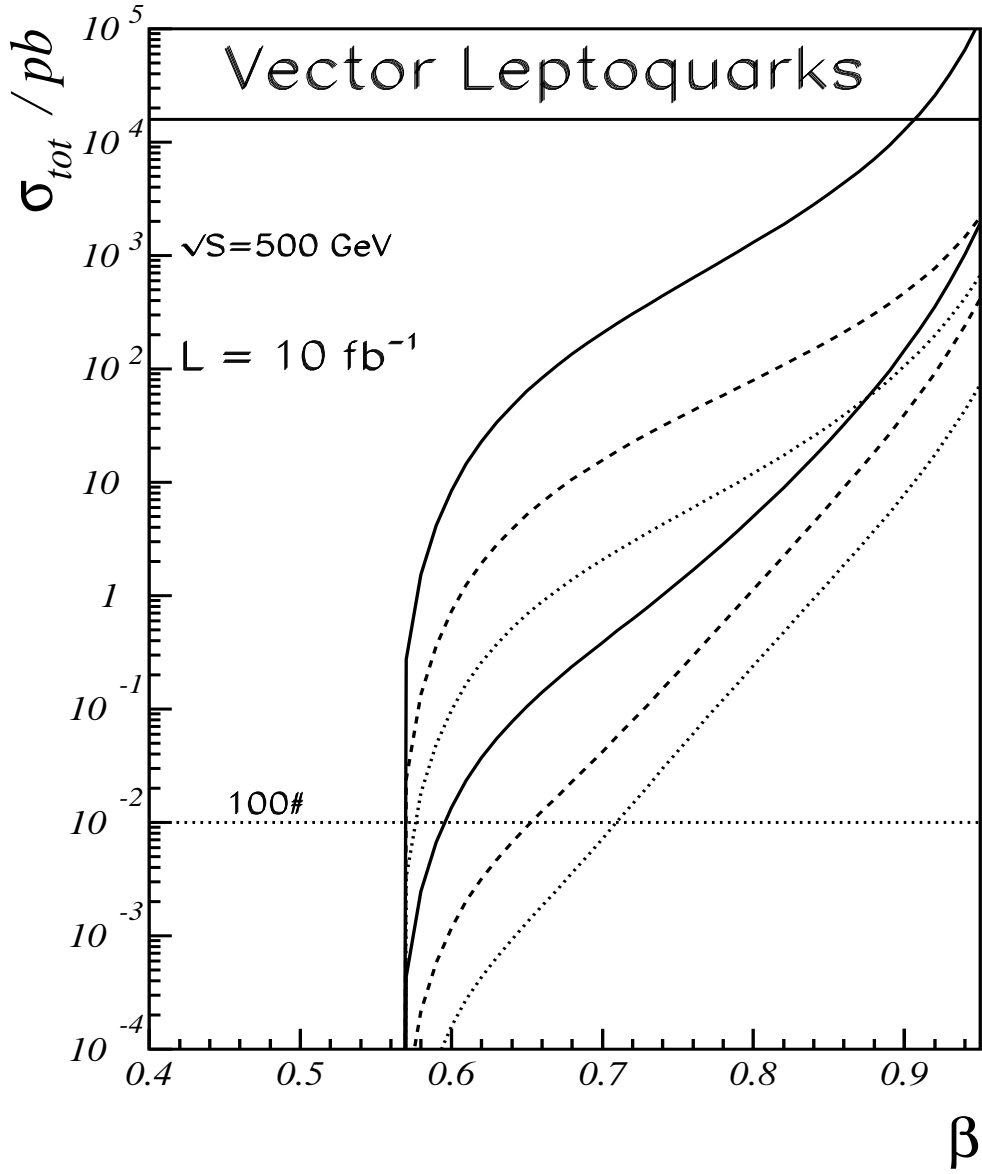


Figure 12b: Integrated cross sections for vector leptoquark pair production at future  $\gamma\gamma$  colliders using laser back scattering for electron beam conversion. The parameters are the same as in figure 12a.